SIMULATION OF THE LONG-TERM SOIL RESPONSE TO ACID DEPOSITION IN VARIOUS BUFFER RANGES

W. DE VRIES

The Winand Staring Centre for Integrated Land, Soil and Water Research, P.O. Box 125, NL-6700 AC Wageningen, The Netherlands

M. POSCH

International Institute for Applied Systems Analysis, A-2361 Laxenburg, Austria

and

J. KÄMÄRI

Water and Environment Research Institute, P.O. Box 250, SF-00101 Helsinki, Finland

(Received April 28, 1989; revised August 9, 1989)

Abstract. A soil acidification model has been developed to estimate long-term chemical changes in soil and soil water in response to changes in atmospheric deposition. Its major outputs include base saturation, pH and the molar Al/BC ratio, where BC stands for divalent base cations. Apart from net uptake and net immobilization of N, the processes accounted for are restricted to geochemical interactions, including weathering of carbonates, silicates and Al oxides and hydroxides, cation exchange and CO_2 equilibriums. First, the model's behavior in the different buffer ranges between pH 7 and pH 3 is evaluated by analyzing the response of an initially calcareous soil of 50 cm depth to a constant high acid load (5000 mol_c ha^{-1} yr^{-1}) over a period of 500 yr. In calcareous soils weathering is fast and the pH remains high (near 7) until the carbonates are exhausted. Results indicate a time lag of about 100 yr for each percent $CaCO_3$ before the pH starts to drop. In non-calcareous soils the response in the range between pH 7 and 4 mainly depends on the initial amount of exchangeable base cations. A decrease in base saturation by H/BC exchange and Al/BC exchange following dissolution of Al^{3+} leads to a strong increase in the Al/BC ratio near pH 4. A further decrease in pH to values near 3.0 does occur when the Al oxides and/or hydroxides are exhausted. The analyses show that this could occur in acid soils within several decades. The buffer mechanisms in the various pH ranges are discussed in relation to Ulrich's concept of buffer ranges. Secondly, the impact of various deposition scenarios on non-calcareous soils is analyzed for a time period of 100 yr. The results indicate that the time lag between reductions in deposition and a decrease in the Al/BC ratio is short. However, substantial reductions up to a final deposition level of 1000 mol_c ha^{-1} yr^{-1} are needed to get Al/BC ratios below a critical value of 1.0.

1. Introduction

Forest canopies can be affected directly by the deposition of SO_2, NO_x and NH_3 but forest ecosystems are also influenced by indirect, soil-mediated effects on the roots. The most notable effect is the inhibition of nutrient uptake (especially of Ca and Mg) either by mobilization of Al (acidification) or by accumulation of ammonium (eutrophication), which leads to unfavorable ratios of these compounds to base cations (Ulrich and Matzner, 1983; Roelofs *et al.*, 1985).

As to acidification, the development of unfavorable ratios of Al to divalent base

Water, Air, and Soil Pollution **48**: 349–390, 1989.

cations strongly depends on the buffer mechanisms of the soil. In highly buffered soils it may take decades or even centuries before measurable changes in this ratio occur, even with high atmospheric deposition, whereas it may take less than a decade in very sensitive soils.

Information on the long-term effects of acid deposition on soils is very important for the formulation of policies for emission reductions. In this respect models provide an important tool to assist decision-makers in evaluating the effectiveness of abatement strategies. Consequently, at the International Institute for Applied Systems Analysis (IIASA) a Regional Acidification Information and Simulation model (RAINS) has been developed that analyzes environmental impacts on a European scale for different emission scenarios. Predictions are based on quantitative descriptions of the linkages between emissions, deposition and environmental impacts such as soil acidification and the effects on terrestrial and aquatic ecosystems (Alcamo *et al.*, 1987). A diagram illustrating the framework and procedure for using RAINS is shown in Figure 1. Similar model systems, mostly on a national level, have been developed in Denmark (Christensen *et al.*, 1985), Finland (Johansson *et al.*, 1989) and the Netherlands (De Vries, 1989).

Within the overall framework of the RAINS model the soil acidification submodel forms an important link between atmospheric deposition and effects on forests, surface waters and groundwater. An earlier version of the soil model, predicting pH as a function of S deposition, has been described in Kauppi *et al.* (1986). This

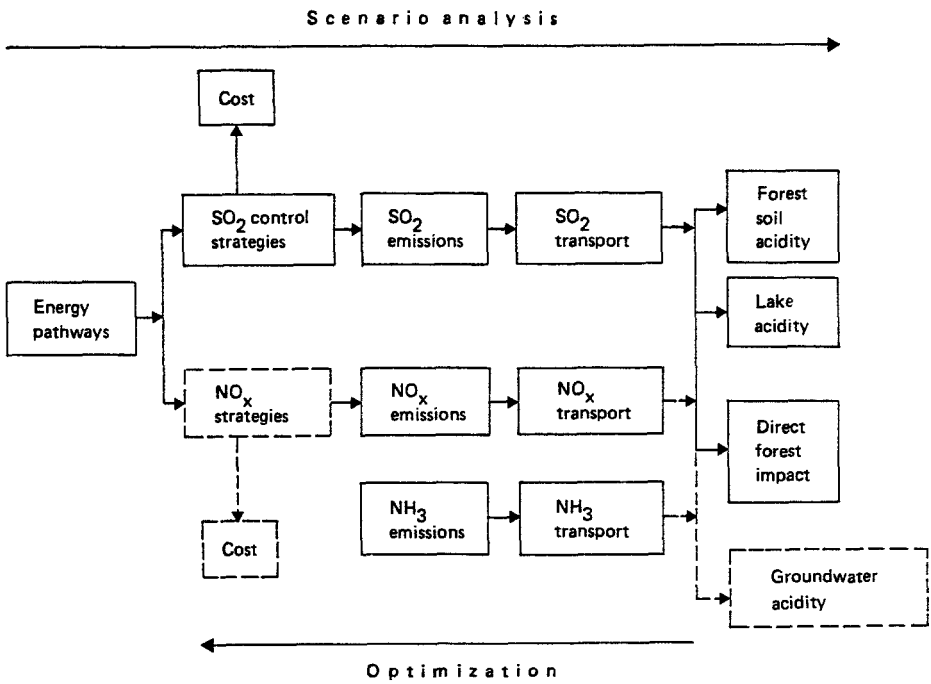

Fig. 1. A schematic overview of the RAINS model.

model was based on the concept of buffer ranges as introduced by Ulrich (1981a, 1983). In this paper we describe a new model called SMART (Simulation Model for Acidification's Regional Trends), which includes the effects of natural soil acidification resulting from the dissociation of CO_2 and the impact of the deposition of NO_x and NH_3. Furthermore, the model predicts not only pH, but all other major components of the soil solution, i.e. Al^{3+}, BC^{2+}, NH_4^+, NO_3^-, SO_4^{2-} and HCO_3^-, because the ratios of A and/or ammonium to divalent base cations (represented by BC^{2+}) are more indicative and sensitive parameters of potential forest damage.

The main objective of SMART is to elucidate the temporal and geographical pattern of forest soil acidification in Europe for alternative emission scenarios. Moreover, national applications of SMART are planned for Finland as part of the Finnish Integrated Acidification Model (HAKOMA) (Johansson *et al.*, 1989). In this context SMART will also be coupled to a lake model (Kämäri, 1988) to analyze lake water acidification in Finland. Agricultural soils will not be included, because normal farming practices such as fertilization, liming and cropping have much greater effects on soil acidity than acidic deposition. This paper focuses on the model's behavior by analyzing the long-term impact of various deposition scenarios on representative forest soils. Special emphasis is put on the model's behavior in the different buffer ranges and the sensitivity of the model output to variations in model input, initial conditions and model parameters. In a subsequent paper we will describe the application of SMART to Europe, focussing on the derivation of data for such a large-scale application. Special emphasis will be given to the use of transfer functions between model parameters and the available data in geographical information systems for soils.

2. Modeling Approach

The objectives of the application of the model strongly determine which approaches are chosen for the modeling, i.e. (see e.g. Kämäri, 1987; De Vries, 1989):

- empirical *vs* process-oriented;
- simple *vs* complex;
- steady state *vs* dynamic; and
- spatially lumped *vs* spatially distributed.

At present, the models for predicting the long-term effects of acid deposition on soils are generally process-oriented, although empirical relationships have sometimes been included, (e.g. Reuss, 1980; Arp, 1983; Chen *et al.*, 1983; Cosby *et al.*, 1985a, b; Bloom and Grigal, 1985; De Vries, 1987) and they have mostly been developed as research tools to elucidate the system's behavior. The reason for developing a new model is that most of these models require a large amount of input data and are therefore not very appropriate for application as management tools at a large regional scale. A notable exception is the model by Bloom and Grigal (1985), but this model does not clearly separate between inputs of SO_2, NO_x and NH_3 and furthermore it uses empirical relationships that were established for soils

in the north-eastern United States.

In order to be able to use the soil model both as a research tool and a management tool we have decided that the model would be:

- process-oriented: to get insight in system's behavior;
- simple: to minimize input data requirements for applications at a regional scale;
- dynamic: to analyze the long-term behavior of soil; and
- spatially distributed: to ascertain the geographical extent of soil acidification.

A special feature of the model is that the spatial distribution of data with respect to soil types is taken into account by using soil maps and relating model parameters to soil survey data using transfer functions (De Vries, 1989).

H^+-transfer in the soil is influenced by numerous reactions (De Vries and Breeuwsma, 1987). In order to minimize input data requirements, when applying SMART for predicting temporal and geographical patterns of forest soil acidification in Europe, the following assumptions have been made:

- The soil solution chemistry depends solely on the net element input from the atmosphere and the geochemical interactions (weathering and cation exchange) in the soil. Apart from the net uptake of N and base cations in harvested plants and the net N immobilization in the forest floor, the influence of the nutrient cycle (foliar exudation, foliar uptake, litterfall, mineralization and root uptake) is not taken into account. This affects model predictions in the root zone (the uppermost 25 to 50 cm). Consequently, in a regional soil acidification model developed for the Netherlands (RESAM), nutrient cycling processes have been included (De Vries, 1989; De Vries and Kros, 1989). However, the amount of data required for this are not available on a European scale. Furthermore, the runoff and leachate concentrations that are important for surface water and groundwater quality are almost unaffected by the exclusion of the influence of the nutrient cycle.
- Sulphate output is in equilibrium with S input. Uptake, immobilization, reduction and adsorption of sulphate are assumed to be negligible. As for adsorption; soils that are high in hydrous oxide minerals can strongly adsorb sulphate, thus reducing cation leaching from soils (Johnson, 1980). However, element budget studies in northern and western Europe (e.g. Rosén, 1982; Van Breemen *et al.*, 1984; Nilsson, 1985) indicate that sulphate adsorption is generally negligible.
- Biological fixation of N and denitrification are negligible. Both assumptions are reasonable for most forest ecosystems (Klemedtson and Svensson, 1988). Notable exceptions are red alder, which has a high rate of N fixation (Van Miegroet and Cole, 1984) and extremely wet forest soils, which have a high rate of denitrification (Tietema and Verstraten, 1989).
- In acid forest soils ($pH < 4.5$), natural soil acidification is ignored. Organic acids can have an appreciable impact in these soils, but the Al that is mobilized by these acids is non-toxic (Ulrich and Matzner, 1983). The formation, complexation and protonation of organic acids has therefore been ignored in the model.
- The weathering rate of base cations from silicates is independent of the soil pH.

This agrees with a thermodynamic analysis of laboratory experiments, which shows that the weathering rate of pure feldspar minerals is pH-independent when the pH varies between 3 and 8 (Helgeson *et al.*, 1984).

- The soil is considered as a homogeneous compartment of constant density. However, it is possible to divide the soil into several layers if this is considered important. In this study a soil depth of 50 cm is assigned, since most biogeochemical interactions occur in this zone.
- The element input mixes completely within the considered soil compartment. This is a reasonable assumption for most forest soils which are well drained and poorly structured (sands, loamy sands and sandy loams). However, in well structured soils with channels and cracks this assumption does not hold. The same is true for hydrophobic soils with preferential flow patterns. Furthermore, it may not be the case in strongly undulating landscapes.
- The water is stationary on a yearly basis, which equals the time step of the model. The reason for this time step is the focus on long-term effects. Seasonal, monthly or even daily fluctuations in soil water chemistry are potentially very important, but the model is developed for predicting trends of increasing probabilities of crucial events.
- The water flux percolating from the top 50 cm of the soil equals the precipitation surplus which equals precipitations minus interception and minus evapotranspiration. Lateral drainage is neglected. This implies that forests obtain all their water from the top 50 cm of the soil. This is a reasonable assumption, because most of the fine roots responsible for water and nutrient uptake occur in this soil compartment.

3. Model Structure

3.1. General

By incorporating the charge balance principle (Reuss *et al.*, 1986) the model structure is based on the anion mobility concept. Figure 2 shows the structure of SMART in a relation diagram. State variables depict the quantities of chemical constituents in minerals (carbonates, silicates and hydroxides) and on the exchange complex, as well as the ion concentrations in the soil solution. Rate variables depict the processes that influence state variables. This includes the net input of elements (deposition minus net uptake and net immobilisation) and water (precipitation minus interception and minus evapotranspiration) and various neutralizing reactions, i.e. the dissolution (weathering) of carbonates, silicates and/or Al hydroxides, and cation exchange.

Table I shows, which ions are included in which processes. The concentrations of SO_4^{2-}, NO_3^-, and NH_4^+ are completely determined by the net element input; the Al^{3+} concentration is controlled by chemical interaction with the soil (weathering and cation exchange) and the concentration of BC^{2+} is regulated by both. Contrary to the leaching of SO_4^{2-}, NO_3^-, and NH_4^+, which is mainly determined by atmospheric

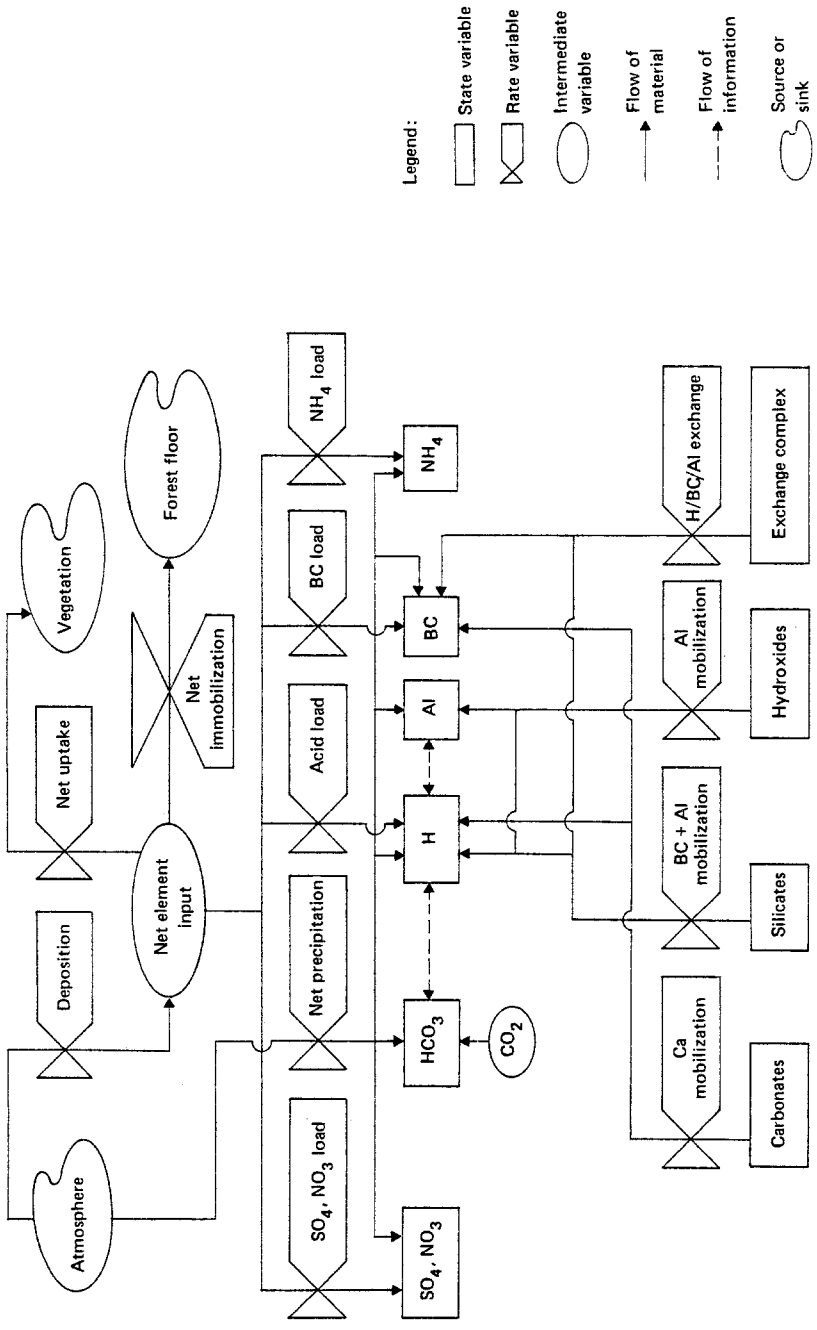

Fig. 2. Relation diagram of SMART (Simulation Model for Acidification's Regional Trends).

TABLE I

Overview of the ions included in the processes in SMART ('+' = ion included in the respective process, '–' = ion not included)

Process	H^+	Al^{3+}	BC^{2+}	NH_4^+	NO_3^-	SO_4^{2-}	HCO_3^-
Atmospheric deposition	+	–	+	+	+	+	–
Uptake	+	–	+	+	+	–	–
Immobilization	+	–	–	+	+	–	–
Nitrification	+	–	–	+	+	–	–
Dissociation/association	+	–	–	–	–	–	+
Carbonate weathering	+	–	+	–	–	–	–
Silicate weathering	+	+	+	–	–	–	–
Al hydroxide weathering	+	+	–	–	–	–	–
Cation exchange	+	+	+	–	–	–	–

deposition, carbonic acid leaching is a natural soil acidification process. The HCO_3^- concentration is based on the assumption of equilibrium with CO_2 content and is regulated by both the CO_2 pressure and the pH. The precipitation surplus affects all ion concentrations. Atmospheric deposition, net removal of N and BC^{2+} by uptake and immobilization and net release of BC^{2+} by silicate weathering are not described by processes, but are required as input to the model. Apart from silicate weathering all neutralization reactions are described by equilibrium reactions. The equilibrium reactions included play a role in specific buffer ranges as defined by Ulrich (1981a, 1983).

In calcareous and slightly acid soils (pH >5), acidity is generated in the soil water by the formation of bicarbonate from dissolved CO_2 and water according to

$$CO_2 + H_2O \rightleftharpoons HCO_3^- + H^+. \tag{1}$$

In calcareous soils the free H^+ produced by this mechanism and by acid input is neutralized by the dissolution of calcite (carbonate buffer range) according to

$$CaCO_3 + H^+ \rightleftharpoons Ca^{2+} + HCO_3^-. \tag{2}$$

Combination of Equations (1) and (2) gives

$$CaCO_3 + CO_2 + H_2O \rightleftharpoons Ca^{2+} + 2HCO_3^-. \tag{3}$$

In non-calcareous soils the H^+ can be neutralized by exchange with divalent cations (exchange buffer range) according to

$$2H^+ + \overline{BC} \rightleftharpoons 2\overline{H} + BC^{2+} \tag{4}$$

where the bar denotes the adsorbed phase. Organic matter has an especially high affinity for H^+, leading to a strong decrease of the effective cation exchange capacity (CEC) with the pH of the soil solution (Helling *et al.*, 1964).

Upon further acidification, a decrease in base saturation will allow H^+ to react with Al in the soil (Al buffer range). This starts to become important below pH

values of about 4.5 (Ulrich, 1981a). In the model we assume that the concentration of Al^{3+} in soil water is in equilibrium with some solid phase of $Al(OH)_3$ according to

$$Al(OH)_3 + 3H^+ \rightleftharpoons Al^{3+} + 3H_2O. \quad (5)$$

In this pH range, cation exchange will not be limited to H/BC exchange, because the exchange sites of the soil matrix have a high affinity for trivalent Al cations, leading to Al/BC exchange according to

$$2Al^{3+} + 3\overline{BC} \rightleftharpoons 2\overline{Al} + 3\,BC^{2+}. \quad (6)$$

However, the amount of Al hydroxides is not infinite and might be exhausted in the topsoil in the near future in areas with high acid deposition rates (Mulder *et al.*, 1989a). When this happens, Fe hydroxides may start interacting with H^+ (Fe buffer range), but the mobilization rate of Fe^{3+} is small in (acid) sandy soils, which are the dominant forest soil types in Europe (De Vries, unpublished laboratory experiments) and has therefore been ignored in the model. In this stage of acidification the Al^{3+}-concentration depends solely on congruent weathering from primary silicates, while there will temporarily be a strong buffering of H^+ by H/Al exchange according to

$$3H^+ + \overline{Al} \rightleftharpoons 3\overline{H} + Al^{3+}. \quad (7)$$

3.2. Process formulations

In the computer code all the model inputs, variables and parameters are abbreviated in a consistent manner. The various abbrevations (prefixes and subscripts) are:

Entity	Constituent	Process	Compartment
F = flux	SO_4^{2-} = sulphate	dep = deposition	carb = carbonates
ct = content	NO_3^- = nitrate	upt = uptake	ox = oxides
K = constant	BC^{2+} = base cations	imm = immobilization	ac = adsorption complex
f = fraction	etc.	nit = nitrification	
		w = weathering	
		dis = dissolution	
		exc = exchange	

Since combinations of constituents with either processes or compartments always refer to fluxes or contents, respectively, the prefixes F and ct are not used in this paper.

Since SMART is based on the charge balance principle, the basic process formulations are close to those of other models based on this principle, such as the Birkenes model (Christophersen *et al.*, 1982), the MAGIC model (Cosby *et al.*, 1985a, b), the ILWAS model (Chen *et al.*, 1983) and the model by Reuss and co-workers (Reuss, 1980, 1983; Reuss and Johnson, 1985).

SMART consists of a set of mass balance equations, which describe the soil

input-output relationships for the cations (Al^{3+}, BC^{2+}, NH_4^+) and strong acid anions (SO_4^{2-}, NO_3^-), and a set of equilibrium equations, which describe the equilibrium soil processes. An explicit mass balance for the ions H^+ and HCO_3^- is not necessary, because these ions have diffuse sources and sinks (dissociation of water, dissolution of CO_2). Their concentration is determined by equilibrium equations and the concentration of the other ions by the charge balance principle

$$[H+] + [Al^{3+}] + [BC^{2+}] + [NH_4^+] = [NO_3^-] + [SO_4^{2-}] + [HCO_3^-]. \quad (8)$$

The concentrations of Na^+, K^+, and Cl^- are not included. It is assumed that they balance each other, since these ion concentrations are mainly regulated by seasalt input.

Mass Balance Equations

For each of the cations (Al^{3+}, BC^{2+}, NH_4^+) and anions (SO_4^{2-}, NO_3^-) considered in SMART a mass balance equation is given by

$$\frac{d}{dt} X_{tot} = X_{in} - PS[X] \quad (9)$$

where X_{tot} = total amount of ion X in the soil ($mol_c m^{-2}$)
X_{in} = net input of ion X to the soil ($mol_c m^{-2}\ yr^{-1}$)
$[X]$ = equivalent concentration of ion X in soil water ($mol_c m^{-3}$)
PS = precipitation surplus ($m\ yr^{-1}$).

The input to the soil system is given by atmospheric deposition. In the model this input is corrected for net uptake and immobilization (NH_4^+, NO_3^-) and net release by weathering of primary minerals. The net input of sulphate, nitrate, ammonium, base cations and Al is calculated according to

$$SO_{4,in}^{2-} = SO_{2,dep} \quad (10)$$

$$NO_{3,in}^- = NO_{x,dep} + f_{nit} NH_{3,dep} - (N_{upt} + N_{imm}) \frac{[NO_3^-]}{[NO_3^-]+[NH_4^+]} \quad (11)$$

$$NH_{4,in}^+ = (1-f_{nit}) NH_{3,dep} - (N_{upt} + N_{imm}) \frac{[NH_4^+]}{[NO_3^-]+[NH_4^+]} \quad (12)$$

$$BC_{in}^{2+} = BC_{dep}^{2+} + T\, BC_w^{2+} - BC_{upt}^{2+} \quad (13)$$

$$Al_{in}^{3+} = T\, Al_w^{3+} \quad (14)$$

where f_{nit} = nitrification factor ($0 \leq f_{nit} \leq 1$).
T = thickness of the soil compartment (m).

The nitrification factor is a lumped parameter which proportions the NH_3 input over NH_4^+ and NO_3^-. If nitrification is not complete ($f_{nit} < 1$), uptake (and immobilization) of both N forms are taken to be proportional to their concentrations. It is implicitly assumed in the model that there is no preference for either NH_4^+ or NO_3^- (see Equations (11) and (12)).

The weathering of Al and base cations are related to each other by

$$Al_w^{3+} = rBC_w^{2+} \tag{15}$$

where r is the stoichiometric ratio of Al^{3+} to BC^{2+} in the congruent weathering of silicates.

The mass balance is applied to the total amounts of ions in the soil. The strong acid anions SO_4^{2-} and NO_3^- do not have an adsorbed phase in the model. Sulphate adsorption is assumed to be negligible (see earlier), whereas nitrate adsorption is insignificant for almost all soil types. Furthermore, the adsorption of NH_4^+ is also ignored, because of the low preference of the exchange complex for this ion in the acid sandy soils (Kleijn *et al.*, 1989), on which most of the forested areas in Europe occur. This can be derived from the fact that acid forest soils in the Netherlands hardly contain NH_4^+ on the adsorption complex, although the concentration of this element in the soil solution can be high, especially in the topsoil, because of the very high NH_3 deposition in this country (Kleijn *et al.*, 1989). For clay soils this assumption is not valid, because fixation of NH_4^+ may play a significant role, but the area of forests on this soils is small. Neglecting adsorption the total amount of SO_4^{2-}, NO_3^-, and NH_4^+ is given by

$$X_{tot} = \Theta\, T[X] \tag{16}$$

where Θ = volumetric waster content of the soil ($m^3\ m^{-3}$).

For base cations in calcareous soils the total amount of ions in the soil is defined as the sum of the amount in the soil solution and in the carbonates. Cation exchange is ignored in this case. This leads to

$$BC_{tot} = \Theta\, T[BC^{2+}] + \rho\, T\, Ca_{carb} \tag{17}$$

where ρ = bulk density of the soil ($g\ cm^{-3}$).
Ca_{carb} = amount of carbonates in the soil ($mmol_c\ kg^{-1}$).

In non-calcareous soils the total amount of base cations is defined as the sum of the amount in the soil solution and at the exchange complex,

$$BC_{tot} = \Theta\, T[BC^{2+}] + \rho T\, fBC_{ac} CEC \tag{18}$$

where fBC_{ac} = fraction of base cations on the adsorption complex.
CEC = cation exchange capacity of the soil ($mmol_c\ kg^{-1}$).

On the other hand, the total amount of Al in these soils is defined as the sum of the amount in soil water, at the exchange complex and in oxides and/or hydroxides. In the various surface water acidification models, such as ILWAS (Chen *et al.*,

1983) and MAGIC (Cosby *et al.*, 1985a, b) the latter amount is assumed to be infinite, but this is not the case in a long-term perspective (De Vries and Kros, 1989; Mulder *et al.*, 1989a). Consequently, the total amount of Al is given by

$$Al_{tot} = \Theta\, T[Al^{3+}] + \rho\, T\, fAl_{ac} CEC + \rho T\, Al_{ox} \tag{19}$$

where fAl_{ac} = exchangeable fraction of Al
Al_{ox} = amount of Al oxides and hydroxides ($mmol_c kg^{-1}$).

When the amount of Al oxides and hydroxides is exhausted ($Al_{ox}=0$), Al_{tot} only refers to the amount in soil water and at the exchange complex.

Equilibrium Equations

The various equilibrium reactions considered in SMART include dissociation of CO_2, dissolution of calcites and Al oxides and/or hydroxides and cation exchange.

The dissociation of CO_2 is calculated according to (see Equation (1))

$$[HCO_3^-][H^+] = K_{CO_2}\, p_{CO_2} \tag{20}$$

where K_{CO_2} is the product of Henry's law constant for the equilibrium between CO_2 in soil water and soil air, and the first dissociation constant, and p_{CO_2} is the partial pressure of CO_2 in the soil.

The dissolution of calcium carbonate (e.g. calcite) is calculated according to (see Equation (3))

$$[Ca^{2+}][HCO_3^-]^2 = K_{carb}\, p_{CO_2} \tag{21}$$

where K_{carb} is the dissolution constant for calcium carbonate.

The dissolution of $Al(OH)_3$ is calculated via (see Equation (5))

$$[Al^{3+}] = K_{gibb}[H^+]^3 \tag{22}$$

where K_{gibb} is the dissolution constant for gibbsite. Actually, the dissolution of Al oxides and/or hydroxides is mainly confined to amorphous material in acid sandy soils (Mulder *et al.*, 1989b; De Vries, unpublished laboratory experiments), whereas gibbsite is generally not found in these soils. However, it is called gibbsite, because field studies have indicated that the dissolution constant for this mineral yields a reasonable prediction of Al in the subsoil (Mulder and Van Breemen, 1987; Cronan *et al.*, 1986).

The various exchange reactions (see Equations (4), (6), and (7)) are described by Gaines-Thomas equations (Gaines and Thomas, 1953) using concentrations instead of activities:

$$\frac{fH_{ac}^2}{fBC_{ac}} = KH_{exc} \frac{[H^+]^2}{[BC^{2+}]} \tag{23}$$

$$\frac{fAl_{ac}^2}{fBC_{ac}^3} = KAl_{exc} \frac{[Al^{3+}]^2}{[BC^{2+}]^3} \tag{24}$$

where KH_{exc} and KAl_{exc} are the Gaines-Thomas selectivity constants for H/BC exchange and Al/BC exchange, respectively. The description of the exchange between H^+ and Al^{3+} is obtained by combining Equations (23) and (24). Since the exchange complex is assumed to comprise H^+, Al^{3+}, and BC^{2+} only, charge balance requires that

$$fH_{ac} + fAl_{ac} + fBC_{ac} = 1. \tag{25}$$

The mathematical procedure for solving this set of mass balance and equilibrium equations as well as the initialization procedures are described in the Appendix.

3.3. Comparison with other models

As stated before, the basis process formulations in SMART are comparable to models such as MAGIC, Birkenes and ILWAS, that are developed to simulate streamwater chemistry by including key soil processes occurring within the catchment. Key soil processes include those described earlier in SMART.

A general review and critique of surface water acidification models has been presented before by Reuss *et al.* (1986) and Kämäri (1987). Apart from soil-oriented charge balance models such as MAGIC, Birkenes and ILWAS, these reviews include empirical charge balance models (Henriksen, 1979; Wright and Henriksen, 1983) and models in which the geochemical buffer processes in the soil are lumped in adsorption isotherms (Arp, 1983) or kinetic expressions (Schnoor *et al.*, 1986).

In order to justify the introduction of a new soil oriented charge balance model, we present a comparison between the processes and process formulations included in SMART and other models based on the charge balance principle (MAGIC, Birkenes and ILWAS). These models are compared with respect to the assumptions made and the goals they are aimed at. Regarding MAGIC and ILWAS, a much more detailed comparison has recently been made by Eary *et al.* (1989).

An overview of the processes and process formulations is given in Table II. There are quite important differences in the modeling philosophy between Birkenes and ILWAS on one hand and SMART and MAGIC on the other hand, influencing the description of hydrological processes. The Birkenes model was originally developed to describe observed streamwater chemistry in the acidified Birkenes catchment in southermost Norway (Christophersen *et al.*, 1982). In this catchment the steamwater chemistry is highly dependent on the flow regime. Since the model was aimed at explaining observed short term trends, a separate two-compartment hydrological submodel has been developed simulating evapotranspiration, quickflow in the upper compartment and base flow in the lower one. In the original Birkenes model snowmelt was not simulated, and predictions were only related to the summer half-year (Christophersen *et al.*, 1982); but in more recent versions a snow reservoir has been included (e.g. Rustad *et al.*, 1986).

Similar to the Birkenes model, ILWAS is also based on the philosophy that confidence in a model must be established by the ability to reproduce short-term dynamics, since long-term calibration data are not available. Consequently, ILWAS

TABLE II

Processes and process formulations included in SMART, MAGIC, Birkenes and ILWAS

Process	SMART	MAGIC	Birkenes	ILWAS
Hydrological processes	Precipitation surplus	Streamflow[a]	Hydrologic submodel	Hydrologic submodel
Biogeochemical processes				
Foliar uptake/exudation	–	–	–	Proportional to: – dry deposition – leaf composition
Litterfall	–	–	–	Model input
Mineralization/ immobilization	Zero order reaction NH_4, NO_3	Zero order reaction[b] NH_4, NO_3, SO_4, Ca, Mg, K, Na	Empirical equation SO_4, BC	First order reaction NH_4, SO_4, Ca, Mg, K, Na
Net uptake	Zero order reaction	Zero order reaction[b]	–	Zero order reaction
Nitrification	Proportional to deposition	Zero order reaction[b]	–	Michaelis Menten kinetics
CO_2-production/ exchange	–	–	–	+
Geochemical processes				
Carbonic acid chemistry	Equilibrium	Equilibria	–[c]	Equilibria
Organic acid chemistry	–	–[d]	–[c]	Equilibria
Carbonate weathering	Equilibrium	–	–	–
Silicate weathering	Zero order reaction (pH-independent)	Zero order reaction (pH-independent)	Zero order reaction (pH-independent)	First order reaction (pH-dependent)
Al hydroxide weathering	Equilibrium	Equilibrium	Equilibrium	Rare limited
Al complexation	–	Equilibria OH, F, SO_4	–	Equilibria OH, F, SO_4
Cation exchange	Gaines-Thomas H, Al, BC	Gaines-Thomas Al, Ca, Mg, K, Na	Gapon H, BC	Gapon H, NH_4, Ca, Mg, K, Na
Anion retention	–	Langmuir SO_4	Linear SO_4	Linear SO_4, H_2PO_4, RCOO

[a] The latest version of MAGIC also contains a hydrological submodel (Eary *et al.*, 1989).
[b] Mineralization, immobilization, (net) uptake and nitrification are specified by net uptake/release fluxes.
[c] A newer version of Birkenes contains an equilibrium equation for HCO_3 and an empirical equation for RCOO (Rustad *et al.*, 1986).
[d] The latest version of MAGIC also contains organic acid equilibria (Eary *et al.*, 1989).

also contains a separate hydrological submodel simulating the various hydrological processes, such as snowmelt, evapotranspiration, partially saturated flow (= quick-flow in the upper compartment of the Birkenes model) and saturated subsurface flow (= base flow in the lower compartment of the Birkenes model). At present, use of the Birkenes model is limited to short-term applications, since it does not contain a mass balance for exchangeable cations, whereas ILWAS can also be used for long-term predictions.

Contrary to Birkenes and ILWAS, the main objective of SMART and MAGIC is to develop a heuristic tool to obtain a conceptual understanding of the long-term responses of soils and catchments to acidic deposition, in order to answer 'what-if' questions by policy makers (scenario analysis). Furthermore, both SMART and MAGIC are based on the assumption that a satisfactory description of the long-term chemical behavior of soils and catchments can be obtained by a lumped representation of the chemical reactions in a homogeneous soil compartment. As far as MAGIC is concerned this implies that the routing of water within the catchment is of less importance. The original MAGIC model thus lacks a detailed hydrological submodel. However, the latest version of MAGIC is a two-compartment model, that runs in conjunction with TOPMODEL (Hornberger *et al.*, 1985), which is a surface hydrology code that provides the hydrologic parameters required by MAGIC-II (Eary *et al.*, 1989). Since SMART is only meant to predict soil acidification, a separate hydrological model has not been included.

As can be seen from Table II, ILWAS is the most complex and detailed acidification model. The major difference to the other models is the explicit inclusion of all major biogeochemical processes affecting soil (and stream) water chemistry, i.e. (1) canopy interactions (foliar uptake and foliar exudation), (2) nutrient cycling (litterfall, mineralization and uptake), (3) N dynamics (nitrification), and (4) CO_2 dynamics (production and exchange). In SMART and MAGIC, canopy interactions and CO_2 dynamics are not simulated, whereas (most of) the other processes are included by simple zero order reactions (model input). Birkenes only contains an empirical equation for the mineralization of SO_4^{2-} as far as biogeochemical processes are concerned.

Similar to the hydrology, the differences between the models can be explained by the goals they are aimed at. ILWAS is meant to reproduce short-term dynamics, which necessitates the explicit inclusion of biogeochemical processes. The same is true for Birkenes, but this model was originally developed for a specific acidified catchment where HCO_3^- and NO_3^- hardly play a role. Consequently, N and CO_2 dynamics have not been included in this model. Attention has been focussed on SO_4^{2-} as the major driving anion. SMART and MAGIC are developed to reproduce long-term changes, which are mainly determined by geochemical processes, such as weathering and cation exchange. Consequently, biogeochemical interactions, such as fluxes due to interactions with the vegetation, simply have to be specified as model input. This also holds for N fluxes due to fixation or denitrification, which are neglected in all the models.

Regarding geochemical processes, ILWAS is again the most detailed model. However, the similarity between the models in this point is rather striking. All models do include the effects of CO_2 dissociation, silicate weathering, Al hydroxide weathering and cation exchange. Apart from ILWAS, all models describe weathering of silicates and Al hydroxides by zero order reactions (fixed amount per time step) and an equilibrium reaction with gibbsite, respectively. In ILWAS both processes are modeled by first order reactions (rate limited), influenced by the pH and the

Al concentration, respectively. Cation exchange is either described by Gaines-Thomas equations (SMART and MAGIC) or by Gapon equations (Birkenes and ILWAS). However, the major difference between the models in this respect is the inclusion of different cations in the exchange equations. In SMART and Birkenes the divalent base cations Ca^{2+} and Mg^{2+} are lumped (BC^{2+}), whereas the monovalent base cations K^+ and Na^+ are excluded, since these ions hardly occur on the exchange complex of most soils. In MAGIC and ILWAS all base cations are included explicitly. Adsorption of NH_4^+ is only considered in ILWAS. Regarding the acid cations, Birkenes and ILWAS include H^+, MAGIC includes Al^{3+}, but SMART is the only model which includes both of them. In our view, this is important, since H/Al exchange may play an important role in strongly acidified soils.

Apart from the inclusion of both H^+ and Al^{3+} in exchange reactions, the major difference between SMART and the other models is the inclusion of carbonate weathering, whereas sulphate adsorption and complexation reactions of Al with RCOO, OH^-, F, and SO_4^{2-} are neglected. Furthermore, SMART contains a mass balance for both carbonates and Al hydroxides. Due to these characteristics SMART is the only model to date, as far as we know, which is able to simulate soil behavior in all buffer ranges.

4. Scenarios and Data

The input data for SMART are summarized in Table III. They have been divided into source/sink terms or system inputs, initial conditions of variables and parameters. System inputs are the atmospheric deposition and the net removal/release fluxes of S, N, base cations and water. With respect to water, the difference between precipitation (deposition) and evapotranspiration (removal) is lumped into one parameter: the precipitation surplus.

The major driving variables (source terms) are the atmospheric deposition of SO_2, NO_x and NH_3. In order to demonstrate the model's behavior, four deposition scenarios were simulated. The deposition levels limiting the various scenarios are given in Table IV; Figure 3 shows the time pattern of the total deposition level for each scenario.

The scenarios start with background levels for SO_2, NO_x and NH_3, that increase to 'European average' levels within 25 yr and stay there for another 25 yr. The 'European average' values are rough estimates based on average throughfall data from 51 sites in Europe (Ivens *et al.*, 1989). Within the next 25 yr deposition levels are reduced by 0, 30, 70, and 90% for scenarios 1, 2, 3, and 4, respectively, and stay there for another 25 yr. The background levels are based on literature information for SO_2 and NO_x (Galloway *et al.*, 1982, 1984) and NH_3 (Asman, 1987). The various reductions are related to political goals and critical loads for various receptors. The 30% reduction refers to the minimal reduction aimed at by most western European countries by the year 1993, a 70% reduction is the political goal in the Netherlands for the year 2015 based on a critical load of 1500 $mol_c\ ha^{-1}$

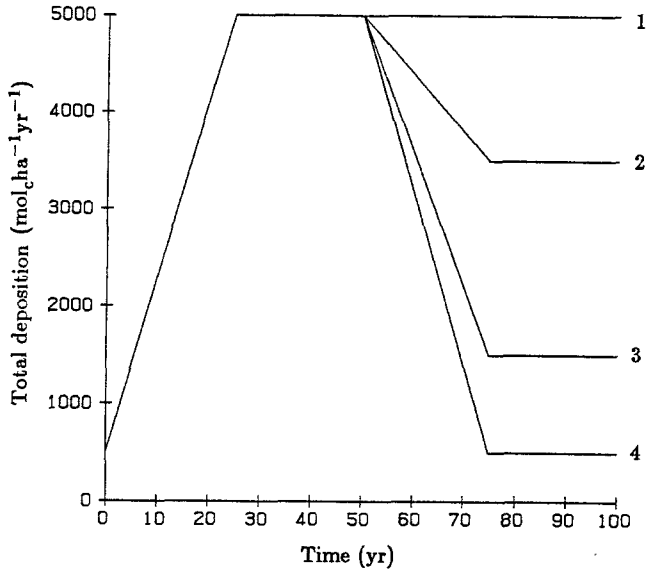

Fig. 3. Temporal trajectories of total deposition levels for four scenarios (see Table IV).

TABLE III

System inputs, variables and parameters used in SMART

System inputs	
Atmospheric deposition:	$SO_{2,dep}$, $NO_{x,dep}$, $NH_{3,dep}$, BC^{2+}_{dep}
Net removal and release in soils:	N_{upt}, N_{imm}, BC^{2+}_{upt}, BC^{2+}_{w}
Precipitation surplus:	PS
Variables	
Ion amounts in solid phases:	$Ca._{carb}$, Al_{ox}
Exchangeable cation fractions:	fH_{ac}, fAl_{ac}, fBC_{ac}
Ion concentrations in solution:	$[H^+]$, $[Al^{3+}]$, $[BC^{2+}]$, $[NH_4^+]$, $[SO_4^{2-}]$, $[NO_3^-]$, $[HCO_3^-]$
Parameters	
Constants:	K_{CO_2}, K_{carb}, K_{gibb}, $K\,Al_{exc}$, KH_{exc}, f_{nit}, r
Soil properties:	ρ, Θ, T, CEC, p_{CO_2}

TABLE IV

Deposition levels of SO_2, NO_x, and NH_3 (in $mol_c\ ha^{-1}\ yr^{-1}$) limiting the different scenarios (see also Fig. 3)

Scenario	Level	SO_2	NO_x	NH_3	Total
1	European average	3000	1000	1000	5000
2	30% reduction	2100	700	700	3500
3	70% reduction	900	300	300	1500
4	Background level	300	100	100	500

yr^{-1} for coniferous forests (De Vries, 1988a), and a 90% reduction might be the ultimate goal to protect the most sensitive surface waters (Hultberg, 1988; De Vries, 1988b). The aim of running simulations with these scenarios was to analyze the influence of various deposition reductions on the rate of recovery of different non-calcareous soils. Furthermore, simulations were made for constant high ('European average') and low (background) deposition levels over 500 yr on an initially calcareous soil, in order to illustrate the model's behavior in the different buffer ranges.

The other model inputs, i.e. the deposition of base cations, the net removal/release fluxes and the precipitation surplus were kept constant over time in all simulations, and their respective values are given in Table V. These data are based on the literature.

The deposition of divalent base cations not balanced by Cl^- varies strongly over Europe. It is generally high near the coast (upper value in Table V), whereas it can be low inland (lower value in Table V). The values are based on data from the Netherlands KNMI/RIVM, 1985) and Scandinavia (Rosén, 1988; Mulder *et al.*, 1989b).

The weathering of base cations varies with the soil type (geological formation). Estimates are based on chemical analyses of soil profiles (Ulrich, 1981b; Fölster, 1985; De Vries and Breeuwsma, 1986), input-output budgets (Van Breemen *et al.*, 1986; Mulder *et al.*, 1987, 1989b) and model calculations (Sverdrup and Warfvinge, 1988a, b). Representative parent rock material (geological formations) related to these data are gneiss for the reference value, schists for the upper value and granites for the lower value (Sverdrup and Warfvinge, 1988a; De Vries, 1988a).

The uptake of base cations and N varies with the tree species and site quality. The data were derived by multiplying the average annual biomass increase of stems, branches and needles by the base cation and N concentrations in the various compartments, assuming whole-tree harvesting. An overview of data related to N uptake can be found in De Vries (1988a). Nitrogen immobilization is taken to be negligible in all simulations.

Contrary to the deposition and weathering of base cations, the model's sensitivity to uptake values was not evaluated, because it is rather obvious. An increase in

TABLE V

Values of model inputs used in the simulations

Variable	Unit	Reference value	Upper value	Lower value
BC^{2+}_{dep}	$mol_c\ ha^{-1}\ yr^{-1}$	400	800	200
BC^{2+}_{w}	$mol_c\ ha^{-1}\ m^{-1}\ yr^{-1}$	500	1000	250
BC^{2+}_{upt}	$mol_c\ ha^{-1}\ yr^{-1}$	400	–	–
N_{upt}	$mol_c\ ha^{-1}\ yr^{-1}$	800	–	–
N_{imm}	$mol_c\ ha^{-1}\ yr^{-1}$	0	–	–
PS	$m\ yr^{-1}$	0.30	0.60	0.15

BC^{2+}_{upt} leads to a decrease in the net input of base cations ($BC^{2+}_{dep} - BC^{2+}_{upt}$), and this is equal to a decrease in BC^{2+}_{dep}. Similarly, an increase in N_{upt} leads to a decrease in acid load, and this is equal to a decrease in N deposition as simulated by the different scenarios.

The annual precipitation surplus, PS, varies significantly over Europe, ranging from less then 100 mm in Mediterranean countries to more than 2000 mm in Scandinavia (Müller, 1982). As a basis for our simulations, 300 mm per year were considered as typical; the upper and lower values cover most of the variation in Europe.

Initial conditions of variables refer to the amount of base cations in calcites and on the exchange complex, as well as the amount of Al oxides and/or hydroxides. The values used in our simulations are given in Table VI.

The initial amounts of calcite and Al oxides and/or hydroxides in the calcareous soil were assumed to be low in order to illustrate the model's behavior in all buffer ranges with the constant high acid input during 500 yr (Al_{ox} is exhausted). The value of Al_{ox} in the non-calcareous soils is an average value for A and B horizons in acid sandy soils, derived from the Dutch soil information system. This value is so high, that the soil stayed in the Al buffer range for 100 yr simulations with the various deposition scenarios (Al_{ox} is not exhausted).

The initial value of fBC_{ac} in nearly all simulations is given in Table VI. The initial values of fH_{ac} and fAl_{ac}, as well as the initial concentrations of H^+, BC^{2+}, and Al^{3+} are derived by combining equilibrium equations in the soil with the charge balance equation. However, in some simulations $fBC_{ac,0}$ is determined by the base cation input (see Equation (13)) using the values given in Table V. Initial concentrations of SO_4^{2-}, NO_3^- and NH_4^+ are determined by the initial values of SO_2, NO_x, and NH_3 deposition, respectively (see Appendix).

The parameters used in the model are constants and soil properties that are assumed to be constant over the simulation period. The values used in the model are given in Table VII. Estimates of the constants K_{carb}, K_{CO_2} and K_{gibb} were derived from the literature (Robie and Waldbaum, 1968; May *et al.*, 1979; Lindsay, 1979). The values for K_{gibb} are representative for natural gibbsite (reference value), microcrystalline gibbsite (upper value) and synthetic gibbsite (lower value). Nitrification is assumed to be complete in all simulations (f_{nit}=1). The stoichiometric

TABLE VI

Values of initial conditions used in the simulations

Variable	Unit	Calcareous soil	Non-calcareous soil		
			Reference value	Upper value	Lower value
Ca_{carb}	%[a]	0.5	0	–	–
Al_{ox}	$mmol_c\ kg^{-1}$	75	150	–	–
fBC_{ac}	–	1.0	0.2	0.4	0.1

[a] 1% Ca_{carb} equals 200 $mmol_c\ kg^{-1}$.

TABLE VII

Values of model parameters used in the simulations

Parameter	Unit	Reference value	Upper value	Lower value
K_{carb}	$(mol\ L^{-1})^3\ atm^{-1}$	$10^{-5.83}$	-	-
K_{CO_2}	$(mol\ L^{-1})^2\ atm^{-1}$	$10^{-7.8}$	-	-
K_{gibb}	$(mol\ L^{-1})^{-2}$	$10^{8.77}$	$10^{9.35}$	$10^{8.11}$
f_{nit}	-	1.0	-	-
r	-	2.0	-	-
KAl_{exc}	$mol\ L^{-1}$	1.0	10.0	0.1
KH_{exc}	$(mol\ L^{-1})^{-1}$	15×10^4	30×10^4	7.5×10^4
ρ	$g\ cm^{-3}$	1.3	-	-
Θ	$m^3\ m^{-3}$	0.3	-	-
CEC	$mmol_c\ kg^{-1}$	50	100	15
p_{CO_2}	atm	0.02	0.04	0.01

ratio of Al to base cations is an average value for Ca-Mg silicates. The exchange constants are calculated from observed ion ratios at the adsorption complex and in soil water at 40 sites (and 4 depths) in acid forest soils (Kleijn and De Vries, 1987; Kleijn *et al.*, 1989). The values for KAl_{exc} are low, although values of a similar order of magnitude have been reported in the literature for sandy topsoils (Bache, 1974). Estimates of the physical soil properties ρ, Θ, and p_{CO_2} are indicative of well-drained sandy soils (Cosby *et al.*, 1985b). The value of Θ refers to the moisture content at field capacity. Actually, the yearly averaged moisture content might be much lower, but the model output is almost insensitive for this parameter. Data given for the CEC refer to pH values of 6.5, because the CEC of organic matter decreases with decreasing pH (Helling *et al.*, 1964). The reference, upper and lower values for CEC are representative respectively for a podzolic soil, an organic-rich loamy soil, and an extremely poor sandy soil, such as the dunes in the Netherlands.

The influence of a constantly high input or a constantly low input was evaluated for the calcareous soils; the impact of the other scenarios was analyzed for the non-calcareous soils (see above). The sensitivity analysis of the model for varying inputs, initial conditions and parameters was mainly restricted to the model's behavior in the different buffer ranges.

5. The Model's Behavior in Various Buffer Ranges

The behavior of SMART in the various buffer ranges was evaluated by analyzing the response of calcareous soils (see Table VI) to a constantly high deposition or a constantly low deposition level for a long time period (500 yr). In this section we emphasize the results of a high acid load. First, results are given of the temporal response in soil pH, and the buffer mechanisms regulating this response are discussed. Secondly, the relationship between pH, base saturation and the Al/BC ratio is discussed and results are given of the effect of parameter variation on the temporal

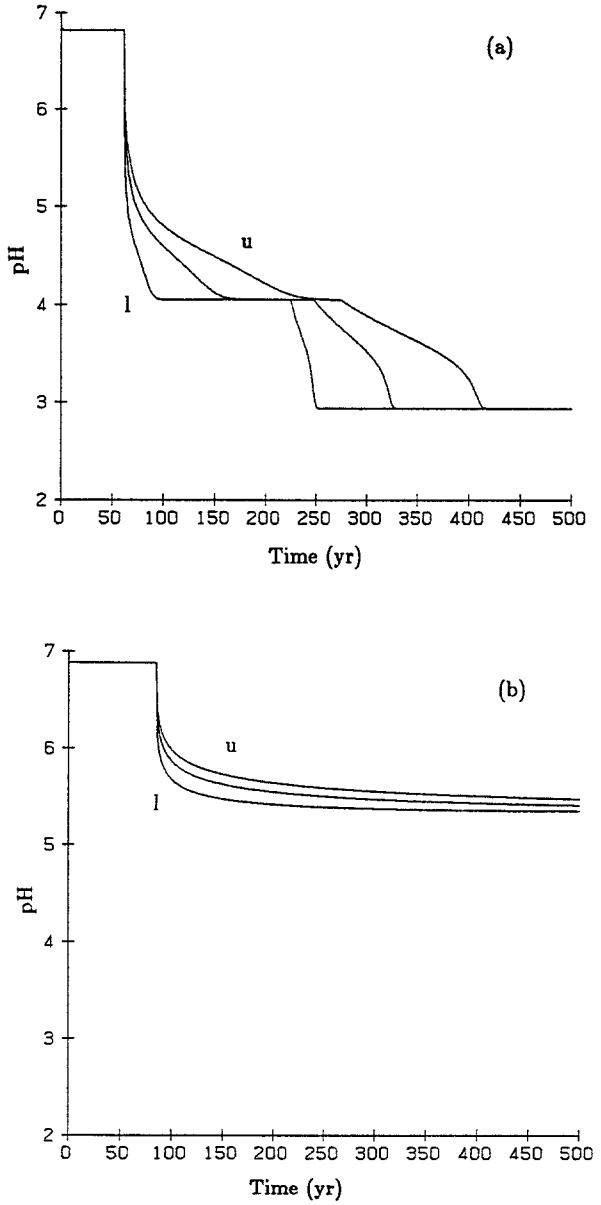

Fig. 4. Time development of the pH for varying CEC values (see Table VII). (a) in response to a constant high acid load, (b) in response to a constant low acid load (background value, see Table IV).

response of pH, base saturation and Al/BC ratio. Here, the Al/BC ratio refers to the molar ratio of inorganic Al to the sum of Ca and Mg, since the role of organic acids is not included in the model. However, effects on soil roots are always related to inorganic Al and not to the total Al (Ulrich and Matzner, 1983).

5.1. Temporal response in soil pH

In Figure 4 the temporal pH trajectories are given for different values of the CEC (see Table VII). For roughly the first 50 yr the soils stay in the carbonate buffer range and the pH remains high. However, as soon as the carbonates are exhausted, there is a sudden drop in pH at high acid loads (Figure 4a), which becomes even more pronounced with decreasing CEC. This is obvious, because the H^+ production in non-calcareous soils is initially mainly neutralized by exchange between H^+ and BC^{2+}, and the buffer capacity of the soil related to this mechanism decreases strongly with decreasing CEC.

The extremely sharp drop in pH for the lower CEC value results from the almost negligible exchange buffer capacity in this poor sandy soil. This leads to an almost direct switch from the carbonate buffer range ($pH \approx 6.8$) to the Al buffer range ($pH \approx 4.0$), because base cation weathering is far too low to neutralize this high acid input. Actually, this predicted sudden drop in pH has been found in dunes in the Netherlands at the boundary of calcareous and decalcified parent material (De Vries, unpublished pH data).

An increase in CEC causes a more gradual decrease in pH, especially in the pH range 5.0 to 4.0, which corresponds to the cation exchange buffer range defined by Ulrich (1981a, 1983). As long as the soil contains Al oxides and/or hydroxides, the pH remains above 4.0, but as soon as these minerals are exhausted, the pH drops further to values near 3.0. Again, this is illustrated most clearly for the poor sandy soil, where the pH drops suddenly, after Al_{ox} has been exhausted. In the other soils, the change is more gradual, because of exchange between H^+ and Al^{3+}. The pH range between 4.0 and 3.0 coincides with the Al buffer range of Ulrich (1981a). However, Ulrich did not explicitly discuss the role of H/Al exchange in this pH range. Apart from exchange, H^+ buffering below pH 4.0 can also be the result of rate-limited dissolution of Al^{3+} from oxides and/or hydroxides (De Vries and Kros, 1988), but this is not considered in SMART.

At a low acid load (Figure 4b) the soil pH finally drops to about 5.5 and remains there in the so-called silicate weathering range (Ulrich, 1981a, 1983). This final equilibrium pH can easily be explained by the fact that the external acid load (300 $mol_c\ ha^{-1}\ yr^{-1}$ because N is taken up by vegetation) is lower than the H^+ consumption by base cation weathering (500 $mol_c\ ha^{-1}\ yr^{-1}$, the upper value of BC_ω^{2+}). Consequently, the soil pH is finally determined by CO_2 equilibriums when H/BC exchange is quantitatively unimportant. This evaluation of the behavior of the model suggests that the concept of buffer ranges as introduced by Ulrich (1981a) and used in the old RAINS soil acidification model (Kauppi *et al.*, 1986) is valid.

5.2. Buffer mechanisms

In order to elucidate the various buffer mechanisms in non-calcareous soils, Figure 5 shows the acid neutralization fluxes as a function of pH and time, using the reference values as model inputs. The buffer mechanisms refer to base cation weathering (i.e. release of base cations by weathering), H^+ adsorption (exchange

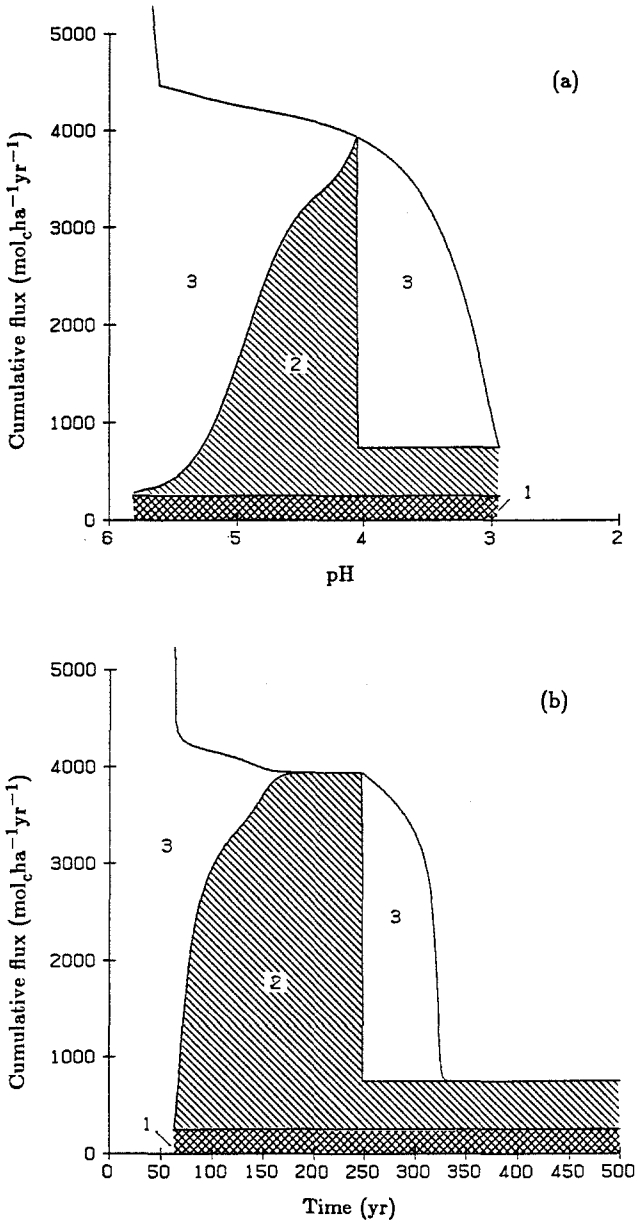

Fig. 5. Cumulative graph of the acid neutralization fluxes, (a) *vs* pH, (b) *vs* time (1 = base cation weathering, 2 = Al^{3+} dissolution, 3 = H^+ adsorption).

against BC^{2+} and Al^{3+}) and Al^{3+} dissolution (by weathering from primary minerals and from hydroxides).

Base cation weathering remains constant over the whole pH range (see assumptions above). Aluminum dissolution is negligible above pH 5.5, because Al released by weathering is precipitated as Al oxide and/or hydroxide (incongruent weathering).

In this range the acid load is almost completely neutralized by exchange between H^+ and BC^{2+} at a rate that is even higher than 5000 $mol_c\ ha^{-1}\ yr^{-1}$ (the external acid load) because of the internal production of H^+ by the dissociation of CO_2. Below pH 5.5, dissolution of Al starts to become an increasingly dominating buffer mechanism. This seems to contradict Ulrich's (1981a) hypothesis that the Al buffer range is between pH 4.2 and 3.0. However, above pH 4.2 the Al, which is dissolved by weathering, is almost completely adsorbed at the exchange complex. Consequently, one might argue that Al dissolution above pH 4.0 to 4.5 is only an internal redistribution of Al^{3+} from hydroxides and silicates to the exchange complex (similar to the redistribution of Al^{3+} from silicates to hydroxides above pH 5.0), whereas depletion of exchangeable base cations is the ultimate buffer mechanism. When the Al oxides and hydroxides are exhausted, the soil pH in the range between pH 4 and 3 is mainly buffered by H/Al exchange. This buffer mechanism has not been described by Ulrich (1981a, 1983), who limits the role of cation exchange to the pH range 5.0 to 4.2. He only refers to Al dissolution in the range between pH 4 and 3. In reality the buffering in acid topsoils (below pH 4) will be regulated both by rate limited Al dissolution from hydroxides and H/Al exchange (De Vries and Kros, 1988).

The redistribution of Al^{3+} in various ranges is shown in Figure 6, which displays the different Al fluxes, i.e. weathering, dissolution and exchange, as a function of pH. The figure illustrates the incongruent weathering above pH 5.0, the Al redistribution from hydroxides to the exchange complex between pH 5.0 and 4.0 and the Al desorption resulting from H/Al exchange below pH 4.0 (compare Figures

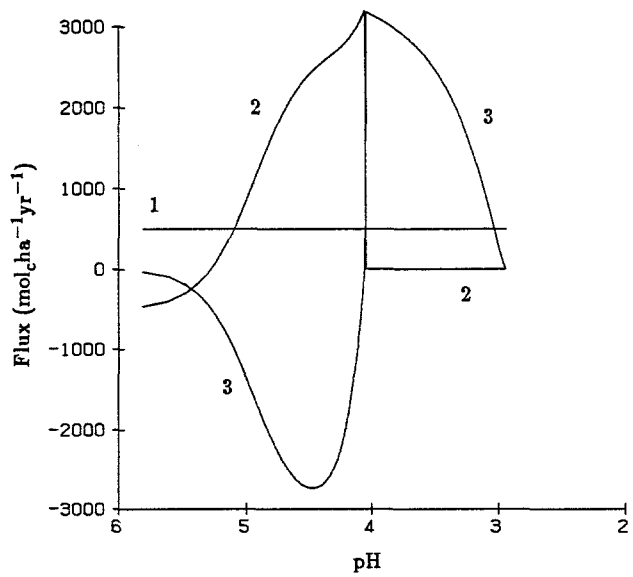

Fig. 6. Aluminum fluxes as a function of pH (1 = weathering from silicates, 2 = weathering from hydroxides, 3 = exchange).

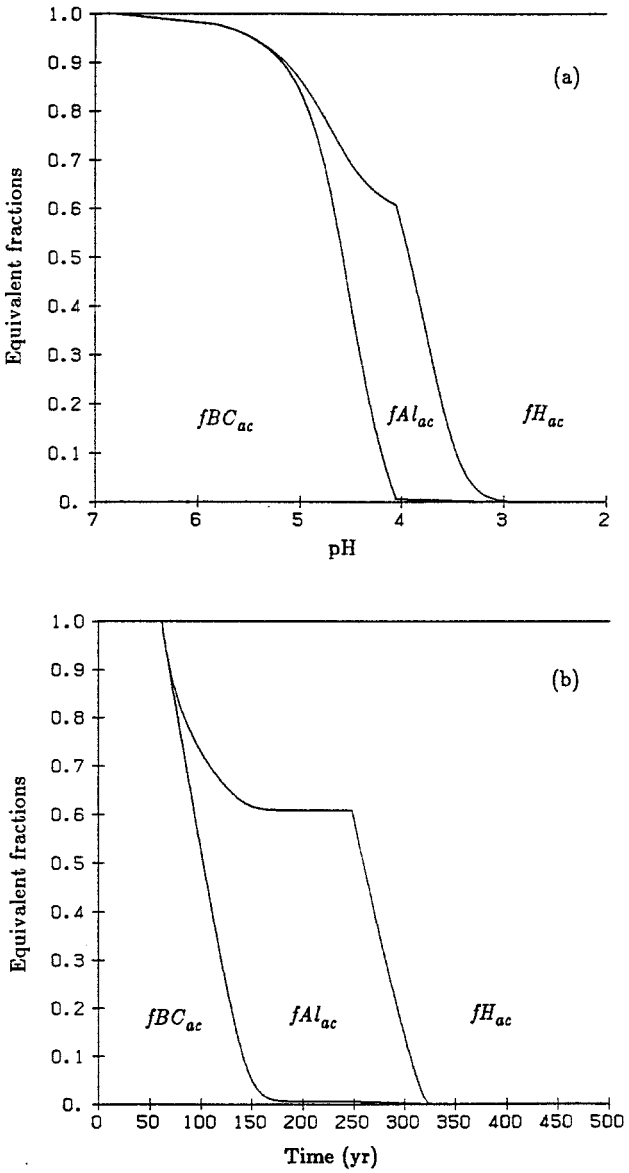

Fig. 7. Exchangeable fractions of BC^{2+}, Al^{3+} and H^+ (a) *vs* pH, (b) *vs* time, using reference values as input data (note that $fBC_{ac} + fAl_{ac} + fH_{ac} = 1$).

5a and 6). As soon as Al_{ox} is exhausted, Al dissolution drops to zero. At that moment the H^+ neutralization is completely compensated by Al^{3+} desorption, which becomes the new buffer mechanism. The system is directly forced into a new equilibrium between H^+ and Al^{3+} on the exchange complex and in the soil solution. Mathematically, the relationship between H^+ and Al^{3+} regulated by dissolution and H/Al exchange is identical.

The role of cation exchange is also illustrated in Figure 7, which shows the exchangeable fractions of BC^{2+}, Al^{3+} and H^+ as a function of pH and time, using the reference values as input data. Figure 7a shows that H^+ adsorption starts near pH 5.5, whereas the increase in Al^{3+} at the adsorption complex starts near pH 5.0. In the Al buffer range the base saturation (fBC_{ac}) decreases to almost zero (near pH 4.0), whereas fH_{ac} and fAl_{ac} are approximately 0.45 and 0.55, respectively. This is consistent with available data for acid forest soils (Kleijn *et al.*, 1989), but it is also to be expected, because the exchange constants were derived from the equivalent fractions of H^+, Al^{3+} and BC^{2+} on the complex and the concentrations of these ions in the solution of these soils (see earlier).

The prediction of an almost negligible base saturation near pH 4.0 is nearly insensitive to the values of the exchange and solubility constants used. However, the exchange constants (KH_{exc}) and the Al^{3+} solubility constant (K_{gibb}) do influence the final values of fH_{ac} (and fAl_{ac}). This is illustrated in the figure in the Appendix, which gives fH_{ac} as a function of a lumped parameter K (see Appendix). An increase in $K=K_{gibb}\sqrt{KAl_{exc}/KH^3_{exc}}$, which might be due to increasing values of K_{gibb} and KAl_{exc} or a decreasing value of KH_{exc}, leads to a lower final value of fH_{ac} (and a higher value of fAl_{ac}). The arrows in the figure refer to the upper, reference and lower values for each of the mentioned constants.

5.3. Relationship between pH, base saturation and Al/BC ratio

As shown before, the response in soil pH between 7 and 4 depends strongly on the base saturation. The relationship between pH and base saturation in this pH range is influenced by the values of the solubility and exchange constants. Furthermore, since pH is strongly related to the Al^{3+} concentration, these constants also affect the relationship between Al^{3+} (and Al/BC ratio) and base saturation. This is illustrated in Figure 8 for varying KAl_{exc}.

The relationship between pH and base saturation shown in Figure 8a is consistent with empirical data given by Clark and Hill (1964) for various soils, especially podzols. An increase in KAl_{exc} yields somewhat higher pH values at the same base saturation, but the effect is not dramatic. The effect of KH_{exc} and K_{gibb} (not shown here) is similar to the one of KAl_{exc}, although the effect of KH_{exc} is more pronounced, especially at higher base saturations (above fBC_{ac}=0.6). The empirical relationship between effective CEC and pH, as found by Helling *et al.* (1964), suggests that H^+ adsorption in soils rich in organic matter might even be much stronger at high pH values. It is likely that in these soils KH_{exc} decreases with a decreasing base saturation (increasing H^+ saturation). In such soils the total removal of Al^{3+} by H^+ in the pH range below 4.0 (when Al_{ox} is exhausted) is questionable.

The relationship between Al/BC ratio and the base saturation (Figure 8b) illustrates the preference of the adsorption complex for Al^{3+} above BC^{2+}. Unless the base saturation is depleted to about 30 to 40%, Al^{3+} does not come into solution. Higher values of KAl_{exc} lead to an even more pronounced shape of the curve. The same is true for KH_{exc} and K_{gibb} although the effect of K_{gibb} is small (not

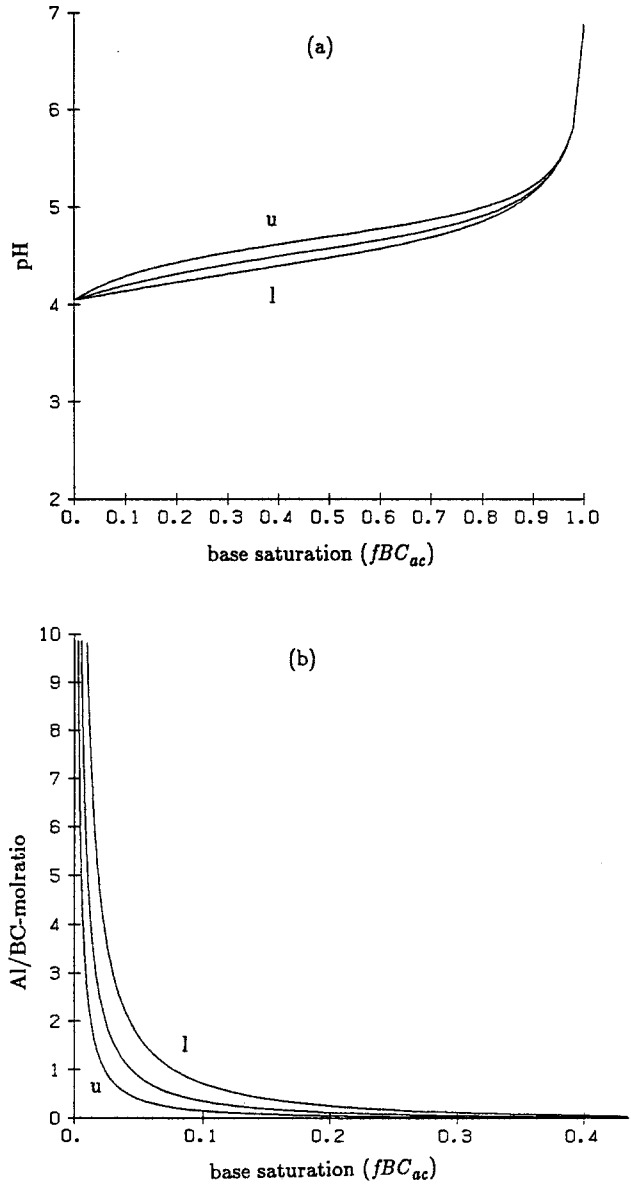

Fig. 8. (a) pH and (b) Al/BC mol ratio *vs* base saturation (fBC_{ac} for varying KAl_{exc} (see Table VII; u = upper value, r = reference value, l = lower value). Note that the values for $Al_{ox} = 0$ are not displayed.

shown here). Similar relationships have been derived by Reuss (1983), using a model including Al dissolution from oxides and/or hydroxides and Al/BC exchange.

Below a base saturation of 5 to 10% (fBC_{ac} = 0.05 to 0.10) the Al/BC ratio increases rapidly (see Figure 8b), whereas the pH is only slightly sensitive to changes in fBC_{ac} in this range (see Figure 8a). This means that the relationship between Al/BC ratio and pH is also very pronounced. Near pH 4.0 a small change in pH

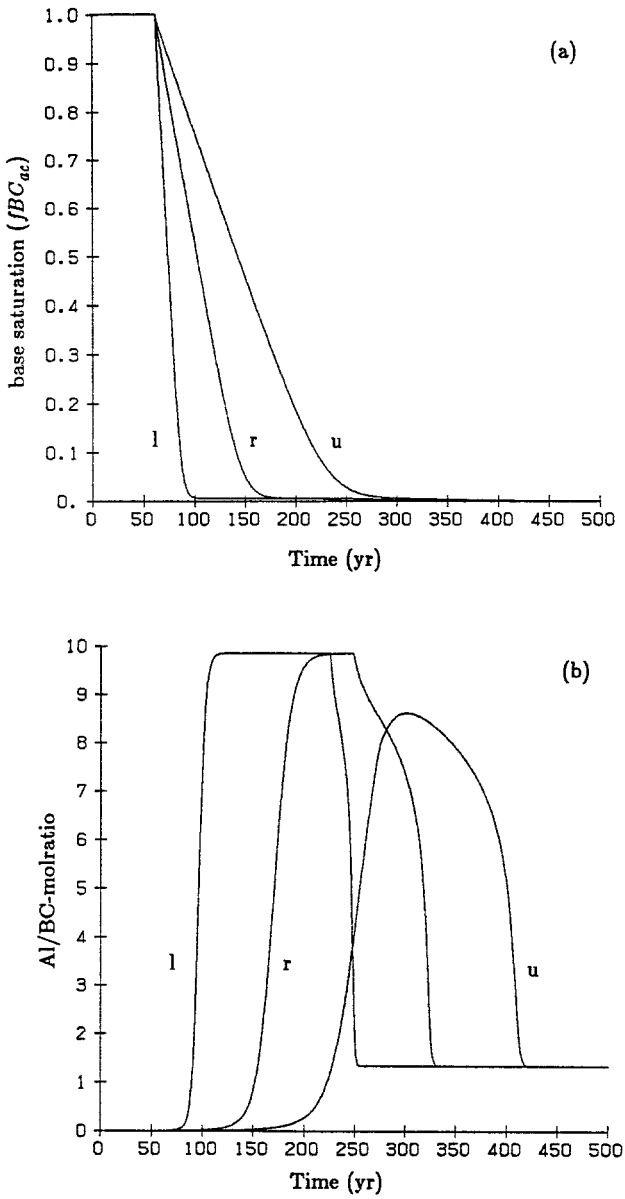

Fig. 9. Time development of (a) base saturation (fBC_{ac}) and (b) Al/BC mol ratio for varying CEC (u = upper value, r = reference value, l = lower value).

causes a dramatic change in the Al/BC ratio. This pH value and the above-mentioned base saturation coincide with a critical Al/BC ratio of 1.0 (Ulrich and Matzner, 1983; Roelofs *et al.*, 1985). However, the Al/BC ratio is a much more sensitive parameter.

5.4. Effects of parameter variation on time lags of pH, base saturation and Al/BC ratio

Contrary to the exchange constants, the CEC does not influence the relationship between pH or Al/BC ratio and base saturation. However, this soil property strongly influences the time development of these variables. This is illustrated in Figure 9. An increase in CEC leads to a longer time period for depleting the exchangeable base cations (see Figure 9a), thus causing a longer time lag before the Al/BC ratio starts to increase (see Figure 9b). The final Al/BC ratio is equal to the stoichiometric weathering ratio (r), because BC^{2+}_{dep} equals BC^{2+}_{upt} (no net input).

The temporal trajectories of pH (Figure 4a) and the Al/BC ratio (Figure 9b) can easily be related to the temporal trajectory of the base saturation (Figure 9a), using the information given in Figure 8 about the relationships of pH and Al/BC ratio with base saturation.

The exchange constants also influence the time development of base saturation, pH and Al/BC ratio. An increase in either KAl_{exc} or KH_{exc} causes a faster depletion of exchangeable base cations, which implies a shorter time period before the Al/BC ratio starts to increase, even though this increase does not occur at a lower base saturation (see Figure 8b). This is illustrated in Figure 10 for KAl_{exc}.

The influence of BC^{2+}_{dep} and BC^{2+}_{w} on the temporal trajectories of pH, Al/BC ratio and base saturation is obvious. An increased input of BC^{2+}, either by deposition or weathering, only slightly affects the trajectories of pH and base saturation, but it causes higher base cation concentrations, leading to significantly lower Al/BC ratios in the Al buffer range (not shown here).

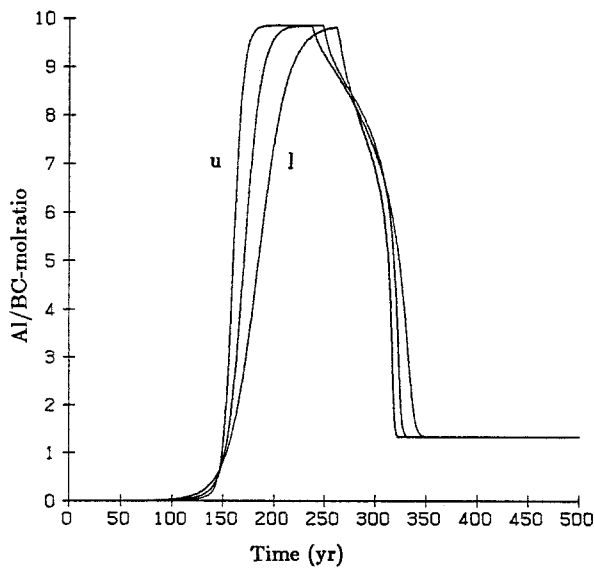

Fig. 10. Time development of the Al/BC mol ratio for varying KAl_{exc} (see Table VII; u = upper value, r = reference value, l lower value).

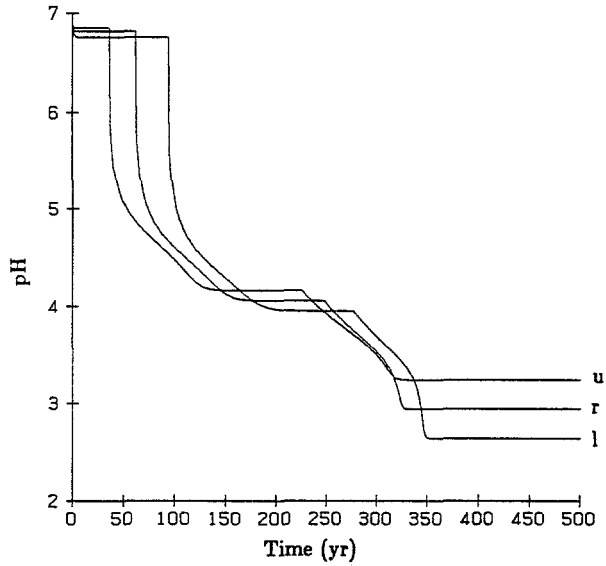

Fig. 11. Time development of pH for varying precipitation surplus (see Table V; u = upper value; r = reference value, l = lower value).

The influence of the precipitation surplus (PS) is also very obvious; a lower PS leads to higher concentrations of H^+ (lower pH), Al^{3+} and BC^{2+}, whereas the Al/BC ratio remains unaffected. However, starting with an initially calcareous soil, a change (e.g. a decrease) in PS also leads to a change (increase) in the duration of carbonate weathering. This causes a time lag in the decrease of pH and base saturation and the increase of the Al/BC ratio. This is illustrated for the pH in Figure 11.

The influence of variations in p_{CO_2} is similar to PS, because a decrease in p_{CO_2} also increases the duration of carbonate weathering. However, at lower pH (below pH 4.5) the influence of variations in p_{CO_2} is negligible.

6. Scenario Analysis

The influence of different deposition scenarios on the temporal evolution of the Al/BC ratio and the base saturation are shown in Figure 12. Here we used the reference values for the initial conditions (CEC = 50 $mmol_c\ kg^{-1}$, $fBC_{ac,0}$ = 0.2) and model parameters. The results of scenario 1 illustrate the considerable time lag between the period of acid deposition increase (25 yr) and Al/BC ratio increase. The time period before the Al/BC ratio becomes critical (above 1.0) is approximately 35 yr (see Figure 12a). This coincides with a base saturation of approximately 5% and is consistent with the relationship between Al/BC ratio and base saturation given earlier (Figure 8b).

The deposition reductions between 50 and 75 yr for scenarios 2, 3, and 4 almost directly influence the predictions of the Al/BC ratio. This is conceivable, because

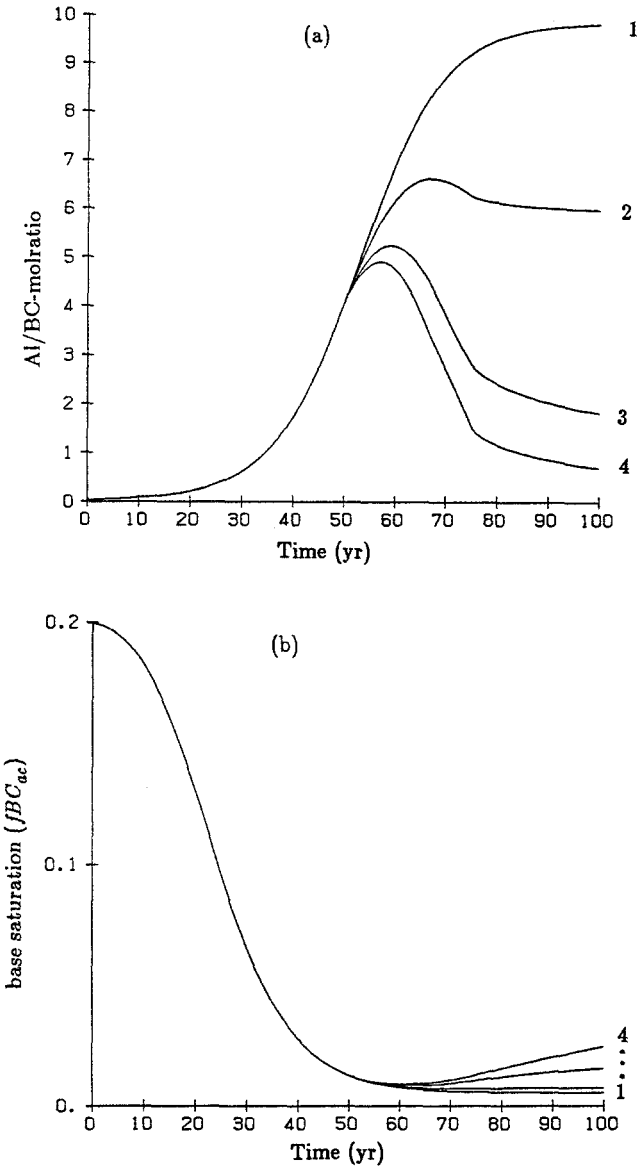

Fig. 12. (a) Al/BC model ratio and (b) base saturation (fBC_{ac}) as a function of time for four deposition scenarios (see Table IV and Figure 3).

a decreased input of S and N directly influences the concentrations of SO_4^{2-} and NO_3^- and, in turn, this directly influences the Al^{3+} concentration (charge balance), because Al dissolution is the dominant buffer mechanism in acid sandy soils. For some soils the time lag might be somewhat longer because of SO_4^{2-} desorption, but this process is not included in the model. Figure 12a shows that a deposition reduction of 30% still leads to an increase in the Al/BC ratio. A reduction of

at least 70% (up to 1000 mol_c ha^{-1} yr^{-1}) is needed to arrive at a final Al/BC ratio of 1.0, but the time taken to achieve this ratio is more than 100 yr (not shown in Figure 12a). However, one should be aware that the nutrient cycle is not included in the model. The Al/BC ratio is completely dependent on geochemical interactions, because the net input of base cations is zero when using the reference values (net uptake equals deposition). Consequently, the predicted ratios will be most reliable for subsoils (e.g. below B-horizons). In the topsoil the Al/BC ratio will be more favorable because of a net input of base cations by deposition and mineralization. Nevertheless, a deposition level of 1000 to 1500 mol_c ha^{-1} yr^{-1} is consistent with critical loads 1400 to 1800 mol_c ha^{-1} yr^{-1} that have been derived for Dutch forest soils in relation to a critical Al/BC ratio of 1.0 for the top 30 cm by using a static soil acidification model including the biocycle (De Vries, 1988a). However, in this model lower values were taken up for N uptake and base cation weathering.

The results of scenario 4 show that the decrease in the Al/BC ratio between 50 and 75 yr is very fast, but the decrease of this ratio at background deposition levels after 75 yr is very slow. It takes hundreds of years to regain the original ratio. This can easily be explained by the pronounced relationship between the Al/BC ratio and base saturation (see Figure 8b). A small increase in base saturation at very low levels (Figure 12b) causes a sharp decline in the Al/BC ratio, but this effect is much less pronounced at higher levels. Furthermore, the 'recovery period' required to regain the original base saturation is always longer than the 'acidification period'. The relatively high net acid input (acid load minus N uptake minus base cation weathering) during the 'acidification period' causes a much faster depletion of exchangeable base cations than the addition of base cations during the 'recovery period' with a very low net acid input. In other words, depletion of exchangeable bases resulting from Al/BC exchange induced by Al dissolution is always faster than the addition of exchangeable bases resulting from BC/Al exchange induced by base cation weathering. This result has also been shown using the MAGIC model (Cosby *et al.*, 1985c).

For a given scenario the temporal trajectory of the Al/BC ratio mainly depends on the initial amount of exchangeable base cations ($fBC_{ac} * CEC$). This is illustrated for scenario 4 for varying CEC (Figure 13a). The time lag between the maximum acid load (after 25 yr) and the maximum Al/BC ratio increases with increasing CEC, but the recovery time is also longer. This is shown most clearly by the difference between the reference CEC and the lower CEC value. In the latter case, changes in the acid load are followed almost immediately by changes in the Al/BC ratio, because the exchange buffer is nearly negligible. Variations in fBC_{ac} are comparable with CEC changes. Apart from initial conditions, the temporal Al/BC trajectory is also influenced by varying exchange constants, because higher constants cause a faster depletion. However, this effect is relatively small (Figure 13b), although it increases with increasing initial base saturation (compare Figure 10).

Variations in precipitation surplus (PS) and partial CO_2 pressure (p_{CO_2}) are

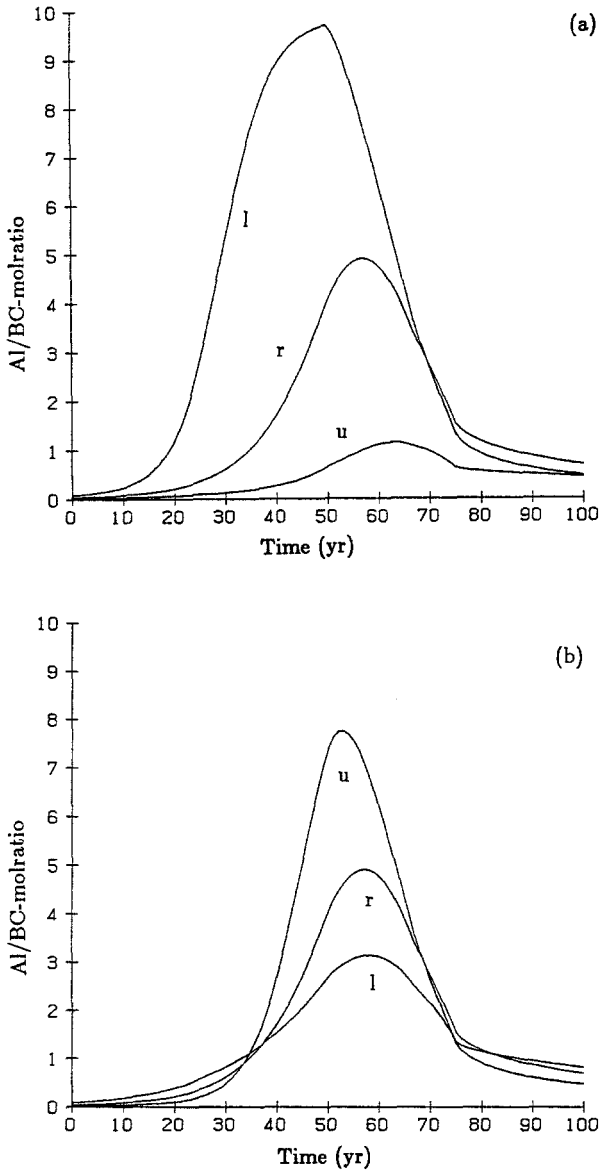

Fig. 13. Al/BC mol ratio *vs* time in response to scenario 4 (90% reduction; see Table IV and Figure 3). (a) for varying CEC, (b) for varying KAl_{exc} (u = upper value, r = reference value, l = lower value).

negligible with respect to changes in base saturation and Al/BC ratio. However, a change in the net input of base cations, either by deposition or by weathering, does influence both output variables. This is illustrated for the Al/BC ratio for varying base cation weathering rates, using scenario 4 (Figure 14a). During the first 20 to 30 yr the effect is small, because of the pronounced relationship between Al/BC ratio and base saturation. However, after 50 yr the Al/BC ratio is significantly

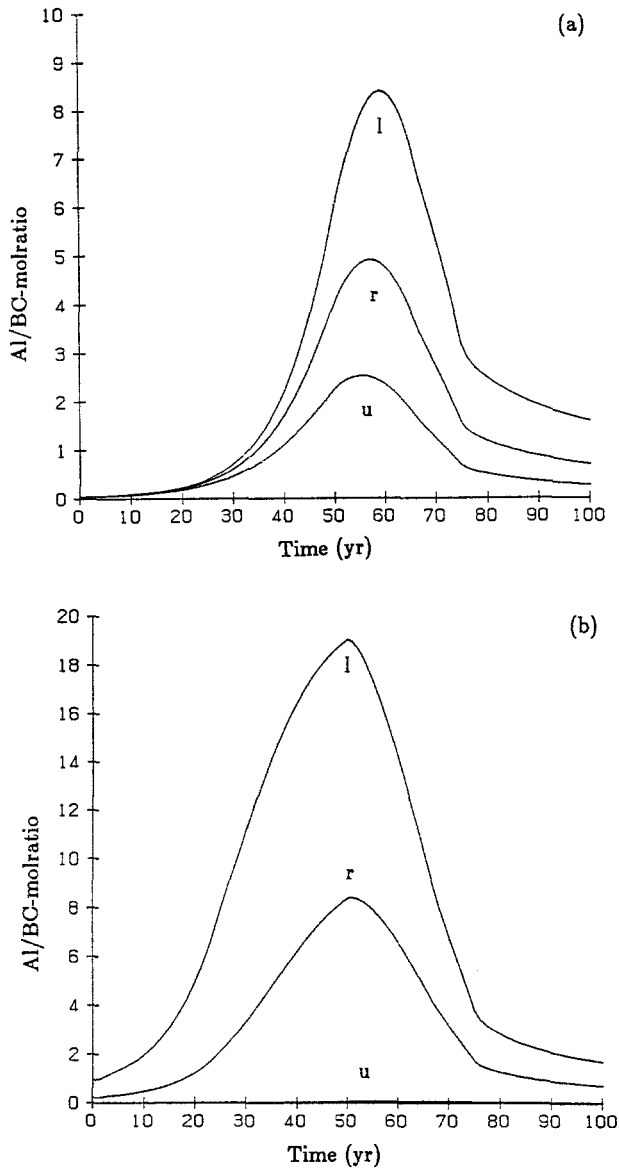

Fig. 14. Al/BC mol ratio *vs* time in response to scenario 4 (90% reduction; see Table IV and Figure 3) for varying base cation weathering rates. (a) initial base saturation $fBC_{ac,0}$ = 0,2, (b) initial base saturation determined by the model (*u* = upper value, *r* = reference value, *l* = lower value).

influenced. This is even more pronounced when one assumes a relationship between base cation weathering and the initial base saturation, as shown in Figure 14b. The initial base saturation is regulated by the initial concentration of BC^{2+}, which depends on deposition, weathering and uptake, and the initial concentration of Al^{3+}, which depends on the background deposition of SO_2, NO_x, and NH_3 and

weathering. Values vary between 80 and 5%. In the first case the Al/BC ratio hardly increases, because the base saturation is only depleted down to 30%. In the last case the Al/BC ratio increases to a value near 20, because the exchangeable bases are nearly exhausted.

7. Conclusions

The results described above are reasonably consistent with Ulrich's concept of buffer ranges characterized by capacities and rates. However, in this concept the role of cation exchange is underestimated. This buffer mechanism does not only occur between pH 5.2 and 4.0, as suggested by Ulrich (1981a), but it plays a role in the entire pH range between 7 and 3.

The soil response depends mainly on its initial conditions. In calcareous soils, weathering is rapid and the pH remains high until the carbonates are exhausted. For a soil layer of 50 cm and a bulk density of 1.3 g cm^{-3}, 1% of $CaCO_3$ corresponds to a buffer capacity of 1300 $kmol_c$ ha^{-1}. This clearly shows that these soils will not become a problem in the near future, although this amount can be exhausted in approximately 100 yr because of the high internal production of H^+ by dissociation of CO_2.

The response of slightly acid soils largely depends on the initial amount of exchangeable base cations. Taking the same layer thickness and bulk density, an average amount of exchangeable BC^{2+} of 15 $mmol_c$ kg^{-1} results in a buffer capacity of approximately 100 $kmol_c$ ha^{-1}. With high acid loads this amount can be exhausted in several decades, as shown by the various simulation results.

A further decrease in pH depends on the amount of Al oxides and/or hydroxides, which in general are abundant. Again, taking the same oil thickness and bulk density, and assuming an average Al_{ox} value of 150 $mmol_c$ kg^{-1}, the buffer capacity equals 975 $kmol_c$ ha^{-1}. This seems an almost infinite amount, as suggested in most of the literature. However, considering a layer thickness of 10 cm only and a high acid input typical for large parts of Western and Eastern Europe, this amount could be exhausted in several decades. This dramatic change in soil chemistry may have serious ecological consequences.

The question of whether the long-term soil responses estimated by SMART are accurate projections of the real system cannot be answered satisfactorily. The model could be verified by comparing simulations of past soil chemistry and soil water chemistry with historical observations, but only few records (e.g. Falkengren-Grerup *et al.*, 1987) extend far enough into the past in order to be suitable for rigorous model testing. However, we can conclude that SMART – including processes that are thought to be most important in influencing soil responses to acidic deposition and using parameter values within ranges appropriate for natural soils – produces plausible results. Even though it cannot be strictly verified for its ultimate use of long-term predictions, it can be used as a tool to obtain a conceptual understanding of long-term soil responses and to make general projections for policy-makers.

Therefore, the model will be linked to RAINS (and eventually to other, similar model systems) to analyze the impact of various emission scenarios on a large (i.e. regional) scale.

Acknowledgments

The manuscript has been critically read by Dr J. Klijn, Dr Ir A. Breeuwsma, and Ir J. Kros. We thankfully acknowledge their useful comments. We also want to thank Dr P. Kauppi for initiating this collaboration and his continuous support.

Appendix: Solution Method

In order to solve the model equation, i.e. to compute the concentrations and total amounts of the various ions, we discretize the mass balance Equation (9). Since we are interested in the long-term development of forest soils, we choose a time step Δt of one year.

For the ions with no internal sources (SO_4^{2-}, NO_3^-, and NH_4^+) Equation (18) applies; replacing the differential operator $d[X]_t/bt$ by its finite difference $([X]_t-[X]_{t-1})/\Delta t$ and rearranging Equation (9) yields

$$[X]_t = \frac{\Theta T[X]_{t-1}+X_{\text{in},t}\Delta t}{\Theta T+PS\Delta t}. \tag{A1}$$

For the sulphate ion the input is given by Equation (10) and (A1) can be solved recursively after defining an initial concentration from the atmospheric input and the precipitation surplus according to

$$[SO_4^{2-}]_0 = \frac{SO_{2,\text{dep},0}}{PS}. \tag{A2}$$

For the nitrate and ammonium concentrations the computation is more complicated, because these concentrations also appear on the right-hand side of Equations (11) and (12). Inserting Equation (A1) into Equations (11) and (12) (for X=NO_3^- and X=NH_4^+, respectively) yields two coupled quadratic equations for $NO_{3,\text{in},t}^-$ and $NH_{4,\text{in},t}^+$, which, because of their special structure, can be solved analytically, yielding

$$NO_{3,\text{in},t}^- = NO_{x,\text{dep},t}+f_{nit}NH_{3,\text{dep},t} - \\ -(N_{\text{upt}}+N_{\text{imm}})\frac{NO_{x,\text{dep},t}+f_{nit}NH_{3,\text{dep},t}+\Theta[NO_3^-]_{t-1}}{NO_{x,\text{dep},t}+NH_{3,\text{dep},t}+\Theta([NO_3^-]_{t-1}+[NH_4^+]_{t-1})} \tag{A3}$$

and

$$NH_{4,\text{in},t}^+ = (1-f_{\text{nit}})NH_{3,\text{dep},t} - \\ -(N_{\text{upt}}+N_{\text{imm}})\frac{(1-f_{nit})NH_{3,\text{dep},t}+\Theta[NH_4^+]_{t-1}}{NO_{x,\text{dep},t}+NH_{3,\text{dep},t}+\Theta([NO_3^-]_{t-1}+[NH_4^+]_{t-1})} \tag{A4}$$

and from these two equations $[NO_3^-]_t$ and $[NH_4^+]_t$ are calculated via Equations (A1). Initial conditions for these ion concentrations are taken as

$$[NO_3^-]_0 = \frac{NO_{x,dep,0} + f_{nit} NH_{3,dep,0}}{PS} \tag{A5}$$

$$[NH_4^+]_0 = \frac{(1 - f_{nit} NH_{3,dep,0}}{PS}. \tag{A6}$$

The solution of the mass balance and equilibrium equations becomes more complicated for the concentrations of base cations and Al.

In *calcareous* soil the concentrations of H^+, BC^{2+} and HCO_3^- are computed from the charge balance equation (Equation (8)) and the two equilibrium equations (Equations (20) and (21))

$$[H^+]_t + [BC^{2+}]_t + [NH_4^+]_t = [NO_3^-]_t + [SO_4^{2-}]_t + [HCO_3^-]_t \tag{A7}$$

$$[HCO_3^-]_t [H^+]_t = K_{CO_2} p_{CO_2} \tag{A8}$$

$$[BC^{2+}]_t [HCO_3^-]_t^2 = K_{carb} p_{CO_2} \tag{A9}$$

where we assume that the concentration of Al is zero in calcareous soils. Denoting the bicarbonate concentration by x, these three equations can be combined to one cubic equation,

$$x^3 + x^2([SO_4^{2-}]_t + [NO_3^-]_t - [NH_4^+]_t) - x K_{CO_2} p_{CO_2} - K_{carb} p_{CO_2} = 0. \tag{A10}$$

To compute the unique positive root of this equation we use Brent's method (Brent, 1973) as documented in Press *et al.* (1986). This method combines the sureness of ordinary bisection algorithms with the speed of a higher order method when appropriate, without using the function's derivative. Once $x = [HCO_3^-]_t$ is computed, $[H^+]_t$ and $[BC^{2+}]_t$ can be calculated from Equations (A8) and (A9).

To obtain the change of the total amount of base cations we rewrite the mass balance equation (Equation (9)) with the aid of Equation (17).

$$\Theta T \frac{d}{dt} [BC^{2+}]_t + \rho T \frac{d}{dt} Ca_{carb,t} = BC_{in,t}^{2+} - PS[BC^{2+}]_t \tag{A11}$$

where $BC_{in,t}^{2+}$ is given by Equation (13), ignoring weathering in calcareous soils,

$$BC_{in,t}^{2+} = BC_{dep,t}^{2+} - BC_{upt}^{2+}. \tag{A12}$$

Discretizing Equation (A11) with a time step of Δt (1 yr), we obtain

$$\rho T\, Ca_{carb,t} = \rho T\, Ca_{carb,t-1} + \Theta T [BC^{2+}]_{t-1} + BC_{in,t}^{2+} \Delta t - (\Theta T + PS\Delta t)[BC^{2+}]_t \tag{A13}$$

where the initial concentration of base cations is taken as

$$[BC^{2+}]_0 = \frac{BC^{2+}_{dep,0} - BC^{2+}_{upt}}{PS}. \quad (A14)$$

Finally, a new value of $BC_{tot,t}$ can be calculated from Equation (17).

For *non-calcareous* soils the charge balance is given by (see Equation (8))

$$[H^+]_t + [Al^{3+}]_t + [BC^{2+}]_t + [NH_4^+]_t = [NO_3^-]_t + [SO_4^{2-}]_t + [HCO_3^-]_t \quad (A15)$$

and the equilibriums considered are (see Equations (20) and (22))

$$[HCO_3^-]_t[H^+]_t = K_{CO_2} p_{CO_2} \quad (A16)$$

and

$$[Al^{3+}]_t = K_{gibb}[H^+]_t^3 . \quad (A17)$$

The change in the total amount of base cations is now given by (see Equations (9) and (18))

$$\Theta\, T \frac{d}{dt}[BC^{2+}]_t + \rho T\, CEC \frac{d}{dt} fBC_{ac,t} = BC^{2+}_{in,t} - PS[BC^{2+}]_t \quad (A18)$$

which, in its discretized form, reads

$$[BC^{2+}]_t = \frac{\Theta T[BC^{2+}]_{t-1} + BC^{2+}_{in,t}\Delta t - \rho T\, CEC(fBC_{ac,t} - fBC_{ac,t-1})}{\Theta T + PS\Delta t} \quad (A19)$$

where the input of base cations is given by (see Equation (13))

$$BC^{2+}_{in,t} = BC^{2+}_{dep,t} + T\, BC^{2+}_{\omega} - BC^{2+}_{upt} . \quad (A20)$$

Furthermore we have the exchange reactions (see Equations (23)-(25))

$$\frac{fH^2_{ac,t}}{fBC_{ac,t}} = KH_{exc} \frac{[H^+]^2_t}{[BC^{2+}]_t} \quad (A21)$$

$$\frac{fAl^2_{ac,t}}{fBC^3_{ac,t}} = KAl_{exc} \frac{[Al^{3+}]^2_t}{[BC^{2+}]^3_t} \quad (A22)$$

$$fH_{ac,t} + fAl_{ac,t} + fBC_{ac,t} = 1. \quad (A23)$$

The solution of this set of equations can be reduced to the solution of a single non-linear equation in $fH_{ac,t}$ in the following way: Inserting $[Al^{3+}]_t$ from Equation (A17) into Equation (A22), taking the third power of Equation (A21), dividing Equation (A22) by the resulting expression and taking the square root yields a relation between $fAl_{ac,t}$ and $fH_{ac,t}$ alone

$$fAl_{ac,t} = K\, fH^3_{ac,t} \quad (A24)$$

with the dimensionless constant K given as

$$K = K_{\text{gibb}} \sqrt{\text{KAl}_{\text{exc}}/\text{KH}^3_{\text{exc}}} \tag{A25}$$

Equation (A23) immediately yields an expression for $\text{fBC}_{\text{ac},t}$

$$\text{fBC}_{\text{ac},t} = 1 - \text{fH}_{\text{ac},t} - \text{K}\,\text{fH}^3_{\text{ac},t}\,. \tag{A26}$$

When $\text{fBC}_{\text{ac}} = 0$, which is generally the case in subsoils of acid forest soils, there is a simple relationship between exchangeable H^+ (fH_{ac}, and its complement fAl_{ac}) and the K value defined by Equation (A25), which is displayed in Figure A1.

Assuming that we know $[\text{BC}^{2+}]_{t-1}$ and $\text{fBC}_{\text{ac},t-1}$ from an initialization procedure or the previous time step, we can express $[\text{BC}^{2+}]_t$ in terms of $\text{fBC}_{\text{ac},t}$ (and therefore $\text{fH}_{\text{ac},t}$) with the aid of the discretized mass balance equation (Equation (A19)). Furthermore, Equation (A21) can be used to express $[\text{H}^+]_t$ as a function of $\text{fH}_{\text{ac},t}$

$$[\text{H}^+]_t = \text{fH}_{\text{ac},t}\left[\frac{[\text{BC}^{2+}]_t}{\text{KH}_{\text{exc}}\,\text{fBC}_{\text{ac},t}}\right]^{1/2}. \tag{A27}$$

Finally, inserting all these expressions for $[\text{HCO}_3^-]_t$ (Equation (A16)), $[\text{Al}^{3+}]_t$ (Equation (A17)), $[\text{BC}^{2+}]_t$ (Equation (A19)) and $[\text{H}^+]_t$ (Equation (A27)) into the charge balance equation (Equation (A15)) yields a single equation for $\text{fH}_{\text{ac},t}$, which can again be solved by Brent's method (see above).

The initialization of this procedure can be done in two different ways, depending on whether the initial value of fBC_{ac} is known or not:
If $\text{fBC}_{\text{ac},0}$ is *not known*, we initialize the concentration of base cations by

$$[\text{BC}^{2+}]_0 = \frac{\text{BC}^{2+}_{\text{dep},0} + T\,\text{BC}^{2+}_{\text{w}} - \text{BC}^{2+}_{\text{upt}}}{\text{PS}}. \tag{A28}$$

Inserting this value into the charge balance equation (Equation (A15)) and using the equilibrium equations (Equations (A16) and (A17)) yields the initial values for the concentrations. Inserting these values into the exchange equations (Equations (A21)-(A23)) allows these equations be solved for the exchangeable fractions.

If, however, $\text{fBC}_{\text{ac},0}$ is known, we can compute $\text{fH}_{\text{ac},0}$ and $\text{fAl}_{\text{ac},0}$ from Equations (26) and (A24), and then use one of the exchange equations together with the charge balance equation and the equilibrium equations to compute the initial concentrations.

Finally, the change in the amount of Al hydroxides is computed by combining the mass balance equation (Equation (9) with Equation (19):

$$\Theta T \frac{\text{d}}{\text{d}t}[\text{Al}^{3+}]_t + \rho T\,\text{CEC}\,\frac{\text{d}}{\text{d}t}\,\text{fAl}_{\text{ac},t} + \rho T \frac{\text{d}}{\text{d}t}\,\text{Al}_{\text{ox},t} = \text{Al}^{3+}_{\text{in},t} - \text{PS}[\text{Al}^{3+}]_t \tag{A29}$$

where $\text{Al}^{3+}_{\text{in},t}$ is given by Equations (14) and (15). Discretizing Equations (A29) we obtain

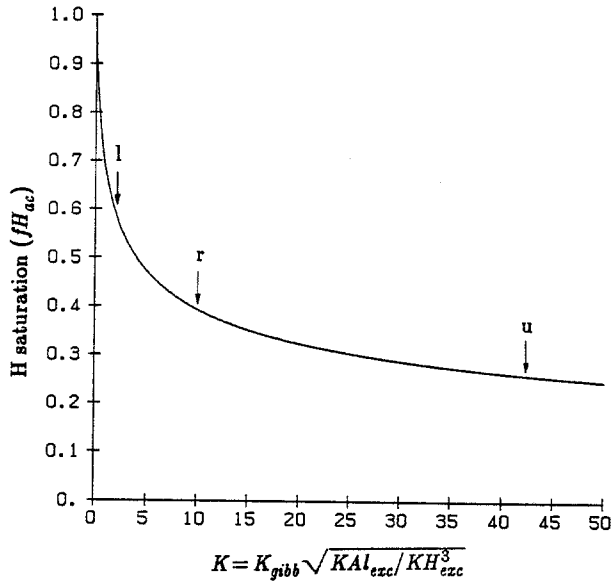

Fig. 15. Relationship between exchangeable H^+ and the dimensionless constant K for zero base saturation (fBC_{ac} = 0; Equations (A25) and (A26)). The arrows refer to the upper reference and lower values of K_{gibb} and the exchange constants (see Table VII).

$$\rho T\, Al_{ox,t} = \rho T\, Al_{ox,t-1} + \Theta T\, [Al^{3+}]_{t-1} + Al^{3+}_{in,t}\Delta t - \\ - (\Theta T + PS\Delta t)[Al^{3+}]_t - \rho T\, CEC(fAl_{ac,t} - fAl_{ac,t-1}). \quad (A30)$$

The value of $Al_{tot,t}$ can then be calculated from Equation (19).

If the amount of Al hydroxides is exhausted, the gibbsite equilibrium reaction no longer occurs and Equation (A24) no longer holds. Therefore, we have to change the solution method, too. Nevertheless, the system of equations can again be reduced to a single non-linear equation, this time in $fBC_{ac,t}$, in the following way:

Putting $Al_{ox,t}$=0 in the discretized form of Equation (A29), we can express $[Al^{3+}]_t$ as a linear function in $fAl_{ac,t}$

$$[Al^{3+}]_t = \frac{\Theta T[Al^{3+}]_{t-1} + Al^{3+}_{in,t}\,\Delta t - \rho T\, CEC(fAl_{ac,t} - fAl_{ac,t-1})}{\Theta T + PS\Delta t}. \quad (A31)$$

In the same way as above, $[BC^{2+}]_t$ can be expressed as a linear function of $fBC_{ac,t}$ (see Equation (A19)). Inserting these two linear expressions into the exchange equation (Equation (A22)) allows us to express $fAl_{ac,t}$ as a function of $fBC_{ac,t}$ alone. From Equation (A23) we then get $fH_{ac,t}$ as a function of $fBC_{ac,t}$. Furthermore, $[H^+]_t$ is given by Equation (A27). Inserting all these expressions into the charge balance equation (Equation (A15)) and using the equilibrium equation (Equation (A16)) yields a single non-linear equation for $fBC_{ac,t}$, which is again solved by Brent's method.

References

Alcamo, J., Amann, M., Hettelingh, J. - P., Holmberg, M., Hordijk, L., Kämäri, J., Kauppi, L., Kauppi, P., Kornai, G., and Mäkelä, A.: 1987, *Ambio* **16**, 232.

Arp, P. A.: 1983, *Ecol. Modelling* **19**, 105.

Asman, W. A. H.: 1987, 'Atmospheric Behaviour of Ammonia and Ammonium', Ph.D. Thesis, Wageningen, The Netherlands.

Bache, B.: 1974, *J. Soil Sci.* **25**, 331.

Bloom, P. R. and Grigal, D. F.: 1985, *J. Environ. Qual.* **14**, 489.

Brent, R. P.: 1973, *Algorithms for Minimization without Derivatives*, Englewood Cliffs, N.J.: Prentice-Hall.

Chen, C. W., Gherini, S. A., Hudson, R. J. M., and Dean, J. D.: 1983, *The Integrated Lake-Watershed Acidification Study. Volume 1: Model principles and application procedures*, EPRI EA-3221, Volume 1, Research Project 1109-5, TETRA TECH INC., Lafayette, California.

Christensen, B., Mortensen, P. B., and Petersen, T.: 1985, *Illustration of the Present Capabilities of the ECCES Program System*, Risø National Laboratory, Denmark: M-2501.

Christophersen, N., Seip, H. M., and Wright, R. F.: 1982, *Wat. Resour. Res.* **18**, 977.

Clark, J. S. and Hill, R. G.: 1964, *Soil Sci. Soc. Am. J.* **28**, 490.

Cosby, B. J., Hornberger, G. M., Galloway, J. N., and Wright, R. F.: 1985a, *Wat. Resour. Res.* **21**, 51.

Cosby, B. J., Wright, R. F., Hornberger, G. M., and Galloway, J. N.: 1985b, *Wat. Resour. Res.* **21**, 1591.

Cosby, B. J., Hornberger, J. M., Galloway, J. N., and Wright, R. F.: 1985c, *Environ. Sci. Technol.* **19**, 1144.

Cronan, C. S., Walker, W. J., and Bloom, P. R.: 1986, *Nature* **324**, 140.

De Vries, W. and Breeuwsma, A.: 1986, *Water, Air, and Soil Pollut.* **28**, 173.

De Vries, W. and Breeuwsma, A.: 1987, *Water, Air, and Soil Pollut.* **35**, 293.

De Vries, W.: 1987, *A Conceptual Model for Analysing Soil and Groundwater Acidification on a Regional Scale*, Proc. Int. Symp. on Acidification and Water Pathways, Vol. I, May 4-8, Bolkesjø, Norway, p. 185.

De Vries, W.: 1988a, *Water, Air, and Soil Pollut.* **42**, 221.

De Vries, W.: 1988b, 'Critical Loads for Sulphur and Nitrogen on Forests, Groundwater and Surface Water', in *Air Pollution in Europe: Environmental Effects, Control Strategies and Policy Options*, Discussion Document for a Conference on Air Pollution, Nörrtalje, September 1988.

De Vries, W.: 1989, 'Philosophy, Structure and Application Methodology of a Soil Acidification Model for the Netherlands', in J. Kämäri (ed.), *Impact Models to Assess Regional Acidification*, Kluwer Academic Publishers, Dordrecht, The Netherlands (in press).

De Vries, W. and Kros, J.: 1989, in J. Kämäri, D. F. Brakke, A. Jenkins, S. A. Norton, and R. F. Wright (eds.), *Regional Acidification Models: Geographic Extent and Time Development*, Springer, New York, p. 113.

Eary, L. E., Jenne, E. A., Vail, L. W., and Girvin, D. C.: 1989, *Archiv. Environ. Contam. Toxicol.* **18**, 29.

Falkengren-Grerup, U., Linnermark, N., and Tyler, G.: 1987, *Chemosphere* **16**, 2239.

Fölster, H.: 1985, in J. I. Brever (ed.), *The Chemistry of Weathering*, Kluwer Acad. Publ., Dordrecht, Holland, p. 197.

Gaines, G. L. and Thomas, H. C.: 1953, *J. Chem. Phys.* **21**, 714.

Galloway, J. N., Likens, G. E., Keene, W. C., and Miller, J. M.: 1982, *J. Geophys. Res.* **87**, 8771.

Galloway, J. N., Likens, G. E., and Hawley, M. E.: 1984, *Science* **226**, 829.

Helgeson, H. C., Murphy, W. M., and Aagaard, P.: 1984, *Geochim. Cosmochim. Acta* **48**, 2405.

Helling, C. S., Chesters, G., and Corey, R. B.: 1964, *Soil Sci. Soc. Am. J.* **28**, 517.

Henriksen, A.: 1979, *Nature* **278**, 542.

Hornberger, G. M., Beven, K. J., Cosby, B. J., and Sappingten, D. E.: 1985, *Wat. Resour. Res.* **21**, 1841.

Hultberg, H.: 1988, in J. Nilsson and P. Grennfelt (eds.), *Critical Loads for Sulphur and Nitrogen*, Miljørapport 1988:15, Nordic Council of Ministers, Copenhagen, Denmark, p. 185.

Ivens, W., Kauppi, P., Alcamo, J., and Posch, M.: 1989, *Sulfur Deposition onto European Forests: Throughfall Data and Model Estimates Tellus* (in press).

Johansson, M., Savolainen, I., and Tähtinen, M.: 1989, in J. Kämäri, D. F. Brakke, A. Jenkins, S.

A. Norton, and R. F. Wright (eds.), *Regional Acidification Models: Geographic Extent and Time Development*, Springer, New York, p. 203.

Johnson, D. W.: 1980, in T. C. Hutchinson and M. Havas (eds.), *Effects of Acid Precipitation on Terrestrial Ecosystems*, Plenum, New York, p. 525.

Kämäri, J.: 1987, *Prediction Models for Acidification*, Proc. Int. Symp. on Acidification and Water Pathways, Vol. I, May 4–8, Bolkesjø, Norway, p. 405.

Kämäri, J.: 1988, 'Regional Lake Acidification Sensitivity and Dynamics', Ph.D. thesis, University of Helsinki.

Kauppi, P., Kämäri, J., Posch, M., Kauppi, L., and Matzner, E.: 1986, *Ecol. Modelling* **33**, 231.

Kleijn, C. E. and De Vries, W.: 1987, in W. van Duijvenbooden and H. G. van Waegening (eds.), *Proc. Int. Conf. on Vulnerability of Soil and Groundwater to Pollutants*, March 30 – April 3, Noordwijk aan Zee, The Netherlands. Proceedings and Information No. 38 TNO-CHO/RIVM, The Hague, p. 591.

Kleijn, C. E., Zuidema, G., and De Vries, W.: 1989, *De indirecte effecten van atmosferische depositie op de vitaliteit van de Nederlandse bossen. 2. Depositie, bodemeigenschappen en bodemvochtsamenstelling van acht Douglasopstanden*, STIBOKA Rapport 2050.

Klemedtson, L. and Svensson, B.H.: 1988, in J. Nilsson and P. Grennfelt (eds.), *Critical Loads for Sulphur and Nitrogen*, Miljørappport 1988:15, Nordic Council of Ministers, Copenhagen, Denmark, p. 343.

KNMI/RIVM: 1985, *Chemische samenstelling van de neerslag over Nederland*, Jaarrapport 1985.

Lindsay, W. L.: 1979, *Chemical Equilibria in Soils*, J. Wiley and Sons, New York.

May, H. M., Helmke, P. A., and Jackson, M. L.: 1979, *Geochim. Cosmochim. Acta* **43**, 861.

Müller, M. J., 1982, *Selected Climatic Data for a Global Set of Standard Stations for Vegetation Science*, Dr. W. Junk Publ., The Hague.

Mulder, J. and Van Breemen, N.: 1987, in T. C. Hutchinson and K. M. Meema (eds.), *Effects of Atmospheric Pollutants on Forests, Wetlands and Agricultural Ecosystems*, Springer Verlag, Berlin-Heidelberg, F. R. G., p. 361.

Mulder, J., Van Grinsven, J. J. M., and Van Breemen, N.: 1987, *Soil Sci. Soc. Am. J.* **51**, 1640.

Mulder, J., Van Breemen, N., and Eijck, H. C.: 1989a, *Nature* **337**, 247.

Mulder, J., Van Breemen, N., Rasmussen, L., and Driscoll, C. T.: 1989b, *Aluminum Chemistry of Acidic Sandy Soils with Various Input of Acidic Deposition in the Netherlands and in Denmark, Geoderma* (submitted).

Nilsson, S. I.: 1985, in F. Andersson and B. Olsson (eds.), *Lake Gårdsjön. An Acid Forest Lake and its Catchment, Ecol. Bulletins* **37**, 311.

Press, W. H., Flannery, B. P., Teukolsky, S. A., and Vetterling, W. T.: 1986, *Numerical Recipes – The Art of Scientific Computing*, Cambridge UP.

Reuss, J. O.: 1980, *Ecol. Modelling* **11**, 15.

Reuss, J. O.: 1983, *J. Environ. Qual.* **12**, 591.

Reuss, J. O. and Johnson, D. W.: 1985, *J. Environ. Qual.* **14**, 26.

Reuss, J. O., Christophersen, N., and Seip, H. M.: 1986, *Water, Air, and Soil Pollut.* **30**, 909.

Robie, R. A. and Waldbaum, D. R.: 1968, *Geol. Surv. Bull.* 1259.

Roelofs, J. G. M., Kempers, A. J., Houdijk, A. L. F. M., and Jansen, J.: 1985, *Plant and Soil* **84**, 45.

Rosén, K.: 1982, *Supply, Loss and Distribution of Nutrients in Three Coniferous Forest Watersheds in Central Sweden*, Reports in Forest Ecology and Forest Soils 41, Swedish University of Agricultural Sciences, Uppsala.

Rosén, K.: 1988, in J. Nilsson and P. Grennfelt (eds.), *Critical Loads for Sulphur and Nitrogen*, Miljørapport 1988:15, Nordic Council of Ministers, Copenhagen, Denmark, p. 269.

Rustad, S., Christophersen, N., Seip, H. M., and Dillon, P. J.: 1986, *Can. J.Fish. Aquat. Sci.* **43**, 625.

Schnoor, J. L., Nikolaidis, N. P., and Glass, S. E.: 1986, *J. Water Pollut. Contr. Fed.* **58**, 139.

Sverdrup, H. U. and Warfvinge, P. G.: 1988a, in J. Nilsson and P. Grennfelt (eds.), *Critical Loads for Sulphur and Nitrogen*, Miljørapport 1988:15, Nordic Council of Ministers, Copenhagen, Denmark, p. 81.

Sverdrup, H. U. and Warfvinge, P. G.: 1988b, in J. Nilsson and P. Grennfelt (eds.), *Critical Loads for Sulphur and Nitrogen*, Miljørapport 1988:15, Nordic Council of Ministers, Copenhagen, Denmark, p. 131.

Tietema, A. and Verstraten, J. M.: 1989, *The Nitrogen Budget of an Oak-beech Forest Ecosystem in the Netherlands in Relation to Atmospheric Deposition*, Dutch Priority Programme on Acidification, Report 04-01.

Ulrich, B.: 1981a, *Z. Pflanzenernähr. Bodenk.* **144**, 647.

Ulrich, B.: 1981b, *Z. Pflanzenernähr. Bodenk.* **144**, 289.

Ulrich, B.: 1983, in B. Ulrich and J. Pankrath (eds.), *Effects of Accumulation of Air Pollutants in Forest Ecosystems*, Kluwer Acad. Publ., Dordrecht, p. 127.

Ulrich, B. and Matzner, E.: 1983, *Abiotische Folgewirkungen der weiträumigen Ausbreitung von Luftverunreinigungen*, Umweltforschungsplan der Bundesminister des Inneren, Forschungsbericht 10402615, BRD.

Van Breemen, N., Driscoll, C. T., and Mulder, J.: 1984, *Nature* **307**, 599.

Van Breemen, N., de Visser, P. H. B., and Van Grinsven, J. J. M.: 1986, *J. Geol. Soc.* **143**, 659.

Van Miegroet, H. and Cole, D. W.: 1984, *J. Environ. Qual.* **13**, 586.

Wright, R. F. and Henriksen, A.: 1983, *Nature* **305**, 422.